Prevention of Ca^{2+}-mediated action potentials in GABAergic local circuit neurones of rat thalamus by a transient K^+ current

H.-C. Pape, T. Budde, R. Mager and Z. F. Kisvárday

Abteilung für Neurophysiologie, Medizinische Fakultät, Ruhr-Universität, D-44780 Bochum, Germany

1. Neurones enzymatically dissociated from the rat dorsal lateral geniculate nucleus (LGN) were identified as GABAergic local circuit *interneurones* and geniculocortical *relay cells*, based upon quantitative analysis of soma profiles, immunohistochemical detection of GABA or glutamic acid decarboxylase, and basic electrogenic behaviour.

2. During whole-cell current-clamp recording, isolated LGN neurones generated firing patterns resembling those in intact tissue, with the most striking difference relating to the presence in relay cells of a Ca^{2+} action potential with a low threshold of activation, capable of triggering fast spikes, and the absence of a regenerative Ca^{2+} response with a low threshold of activation in local circuit cells.

3. Whole-cell voltage-clamp experiments demonstrated that both classes of LGN neurones possess at least two voltage-dependent membrane currents which operate in a range of membrane potentials negative to the threshold for generation of Na^+–K^+-mediated spikes: the T-type Ca^{2+} current (I_T) and an A-type K^+ current (I_A). Taking into account the differences in membrane surface area, the average size of I_T was similar in the two types of neurones, and interneurones possessed a slightly larger A-conductance.

4. In local circuit neurones, the ranges of steady-state inactivation and activation of I_T and I_A were largely overlapping ($V_H = -81{\cdot}1$ *vs.* $-82{\cdot}8$ mV), both currents activated at around -70 mV, and they rapidly increased in amplitude with further depolarization. In relay cells, the inactivation curve of I_T was negatively shifted along the voltage axis by about 20 mV compared with that of I_A ($V_h = -86{\cdot}1$ *vs.* $-69{\cdot}2$ mV), and the activation threshold for I_T (at -80 mV) was 20 mV more negative than that for I_A. In interneurones, the activation range of I_T was shifted to values more positive than that in relay cells ($V_h = -54{\cdot}9$ *vs.* $-64{\cdot}5$ mV), whereas the activation range of I_A was more negative ($V_h = -25{\cdot}2$ *vs.* $-14{\cdot}5$ mV).

5. Under whole-cell voltage-clamp conditions that allowed the combined activation of Ca^{2+} and K^+ currents, depolarizing voltage steps from -110 mV evoked inward currents resembling I_T in relay cells and small outward currents indicative of I_A in local circuit neurones. After blockade of I_A with 4-aminopyridine (4-AP), the same pulse protocol produced I_T in both types of neurones. Under current clamp, 4-AP unmasked a regenerative membrane depolarization with a low threshold of activation capable of triggering fast spikes in local circuit neurones. In relay cells, 4-AP increased the amplitude and duration of the Ca^{2+} action potential.

6. It is concluded that the voltage-dependent properties of I_T and I_A are delicately balanced in the two types of LGN neurones; in relay cells, the balance is shifted towards I_T and production of a low-threshold Ca^{2+} action potential, and I_A contributes to shaping the form of the regenerative depolarization; in local circuit neurones, the properties of I_T and I_A are widely overlapping, resulting in a functional compensation in terms of net membrane current, such that a regenerative Ca^{2+} response is prevented.

The vast majority of sensory signals entering the mammalian central nervous system are relayed through the thalamus on the way to the cortex (Jones, 1985). There is an accumulation of evidence indicating that thalamic nuclei are not merely functioning as relay stations for the transmission of afferent impulses, but are also intimately involved in the process of gating and modulating sensory information during the various global states of functional activity in the brain (for a recent review, see Steriade, Jones & Llinás, 1990). This integrative function of the thalamus relies heavily upon the intrinsic properties of the cortically projecting relay neurones, the level of activity of extrathalamic input systems, and the presence of an intricate local network of synaptic contacts. One prominent element in the local synaptic circuitry is provided by interneurones, which locally ramify within the boundaries of the specific thalamic nucleus and contain the inhibitory transmitter γ-aminobutyric acid (GABA). The relative proportion of interneurones varies between different thalamic nuclei and among species (for a review see Jones, 1985). The dorsal lateral geniculate nucleus (LGN), the main thalamic station of the visual pathway, offers a great advantage for the study of local circuit neurones because the interneurones constitute a distinct group of cells in the LGN, comprising about 20–25% of the total neuronal population (Guillery, 1966), and there is compelling evidence that all interneurones are GABAergic in this nucleus in cat and rodents (Sterling & Davis, 1980; Ohara, Lieberman, Hunt & Wu, 1983; Fitzpatrick, Penny & Schmechel, 1984; Montero & Singer, 1985; Gabbott, Somogyi, Steward & Hamori, 1986). The GABAergic interneurones in the LGN have been morphologically characterized and their synaptic contacts have been quantitatively analysed at the light and electron microscope level (see Discussion).

Despite the wealth of data regarding the morphology and the synaptic connectivity of GABAergic interneurones in the LGN, our understanding of their electrophysiological properties and functional significance is mostly based upon indirect evidence emerging from their action on cortically projecting relay neurones (for a review see Crunelli & Leresche, 1991). Few studies have been more directly related to the physiological properties of intrageniculate interneurones. Using extracellular recording techniques in the rat and cat LGN *in vivo*, presumed interneurones were distinguished from geniculocortical cells through the synaptic delay and the discharge patterns in response to stimulation of the visual cortex, the brainstem or the optic nerve. Interneurones were found to receive monosynaptic excitation from retinal ganglion cells and to possess receptive field properties that resemble those of relay neurones (Burke & Sefton, 1966; Dubin & Cleland, 1977; Ahlsén, Lindström & Lo, 1984). While there is as yet no evidence of any completely identified thalamic local circuit cell recorded *in vivo* that describes its physiological properties (Steriade *et al.* 1990), an intracellular study in the cat LGN *in vitro* demonstrated that morphologically characterized local circuit cells can be distinguished from relay neurones by the short duration of Na^+–K^+-mediated spikes and the ability to generate high-frequency trains of action potentials (McCormick & Pape, 1988). A striking difference between the two classes of neurones relates to the presence of an action potential with a low threshold of activation (Jahnsen & Llinás, 1984*a*, *b*; Steriade & Deschênes, 1984), generated by a transient membrane Ca^{2+} current, I_T (Coulter, Huguenard & Prince, 1989; Crunelli, Lightowler & Pollard, 1989; Hernández-Cruz & Pape, 1989; Suzuki & Rogawski, 1989). In thalamocortical relay neurones, the Ca^{2+} action potential is capable of triggering a burst of fast spikes, thereby providing an important mechanism that contributes to the generation of rhythmic oscillatory bursting of thalamocortical circuits during periods of a synchronized electroencephalogram (as reviewed by Steriade *et al.* 1990; McCormick, 1992). Local circuit neurones, by comparison, were found to lack the typical low-threshold Ca^{2+} action potential (McCormick & Pape, 1988), although earlier studies reported the occurrence of long bursts of spikes in presumed intrageniculate interneurones (Burke & Sefton, 1966).

The present study was undertaken to examine the intrinsic membrane properties of GABAergic local circuit neurones in general, and to evaluate the basis for the differences in low-threshold regenerative Ca^{2+} responses between interneurones and relay cells in particular, which can be assumed to shape their distinctive role within the integrative function of the thalamus. The relative paucity of basic information available on the cellular physiology of local circuit neurones in the thalamus is partly related to their small number and their small soma size, which makes it difficult to encounter, to reliably identify and to physiologically characterize these neurones using standard recording techniques in a multicellular preparation. Therefore in the present study we decided (i) to use the GABAergic local circuit neurones of the rat LGN, which represent a distinctive, morphologically and immunohistochemically well-characterized, neuronal population, (ii) to acutely isolate the neurones from the intact environment of the LGN, (iii) to identify the local circuit interneurones after isolation through morphological analysis, combined with immunohistochemical demonstration of the intrinsic presence of GABA or glutamic acid decarboxylase (GAD), (iv) to quantitatively examine the electrical membrane properties of isolated and identified interneurones using the whole-cell version of the patch-clamp technique (Hamill, Marty, Neher, Sakmann & Sigworth, 1981), and (v) to compare the analysed electrophysiological properties of identified interneurones with those of geniculocortical relay cells. The results provide evidence indicating that acutely isolated local circuit neurones and relay cells from the rat LGN generate patterns of electrical activity that largely resemble those observed in intact tissue, and that

the characteristics of two voltage-gated membrane currents, the T-type Ca^{2+} inward current and the A-type K^+ outward current, account for some of the basic differences in the electrogenic behaviour between the two types of neurones. In particular, the properties of the two membrane currents seem to be delicately balanced, allowing for a distinctive functional interaction, such that the generation of regenerative low-threshold Ca^{2+} responses is promoted in relay cells and prevented under normal conditions in local circuit neurones.

METHODS

Rats of either sex (postnatal days 14–25) were deeply anaesthetized with halothane and decapitated. A block of tissue containing the LGN was removed and placed in 5 °C physiological saline, containing (mM): NaCl, 126; KCl, 2·5; $MgSO_4$, 2; NaH_2PO_4, 1·25; $NaHCO_3$, 26; $CaCl_2$, 2; dextrose, 10. Perfusion of 95% O_2 and 5% CO_2 yielded a pH of 7·4. LGN slices (400 μm) were prepared as coronal sections on a vibratome (Model 1000, Ted Pella, Redding, CA, USA)

Acute isolation of thalamic neurones

Neurones were isolated from LGN slices via an enzymatic dissociation procedure as described previously (Budde, Mager & Pape, 1992; see also Kay & Wong, 1986). Briefly, LGN slices were incubated for 60–90 min at room temperature in oxygenated piperazine-*N*,*N*′-bis(ethanesulphonic acid) (Pipes)-buffered medium containing trypsin (Type XI, Sigma, Deisenhofen, Germany; 1–4 mg ml^{-1}), bovine serum albumin (0·5 mg ml^{-1}) and (mM): NaCl, 120; KCl, 5; $MgCl_2$, 1; $CaCl_2$, 1; Pipes, 20; dextrose, 25; pH adjusted to 7·35 with NaOH. After washing with enzyme-free medium, single neurones were dissociated by titurating a slice with a series of fire-polished, silicone-coated Pasteur pipettes of decreasing tip diameter.

Immunohistochemistry and soma area measurement in isolated LGN cells

A suspension of isolated cells was poured onto gelatine-coated glass slides, immersed into a fixative containing 2% paraformaldehyde (Merck, Darmstadt, Germany) and 0·5% glutaraldehyde (Merck) in 0·1 M phosphate-buffered physiological saline (PBS, pH 7·4), and rinsed in PBS followed by 0·05 M Tris-buffered saline containing 0·05% Triton X-100 (Sigma, TBS-T). In order to reduce unspecific immunostaining, 5% normal pig serum (DAKO GmbH, Hamburg, Germany) was applied for 45 min, followed by the primary antiserum for GABA (Sigma, 1:1000–1:10000, 24 h at 4 °C), the secondary antiserum of biotinylated goat anti-rabbit Ig (Vector Labs, Burlingame, CA, USA; 1:200, 24 h at 24 °C), and the avidin–biotin-complexed horseradish peroxidase (ABC, Vector, 1:200, 24 h at 4 °C). Between steps, slides were rinsed in TBS-T, and the same solution was used for diluting immunoreagents. Immunohistochemical reaction was completed with 0·05% 3,3′-diaminobenzidine.4HCl (DAB, Sigma) by adding 5 μl of 1% H_2O_2 to every 1 ml of the incubating medium. Each slide was dehydrated and coverslipped in DPX mounting medium (Serva, Heidelberg, Germany). The immunohistochemical procedure for the detection of GAD was identical to that of GABA, except that a primary antibody to GAD (kindly provided by W. H. Oertel, München, Germany), a fixative containing 4% paraformaldehyde (Merck), a blocking serum of 5% normal donkey serum (Sigma), and a secondary antiserum of biotinylated donkey anti-sheep Ig (Vector, 1:200) were used.

One of our main interests was to determine whether GABAergic neurones constitute a distinct group of cells in a population of isolated neurones from the LGN. Therefore the somatic areas of three groups of cells were compared: (i) acutely dissociated 'living' cells, (ii) isolated cells immunostained for GABA or GAD, and (iii) isolated cells stained for Nissl substance. Somata of each group were drawn using a light microscope with a ×100 oil objective fitted to a drawing tube. The two-dimensional soma profile of the cells was analysed and digitized into an IBM AT computer with the aid of Bioquant System IV software (R&M Biometrics, Nashville, TN, USA). Shrinkage occurred during immunohistochemical procedures and Nissl staining of the somata of isolated cells. For a direct comparison of these groups of cells with living cells, a correction factor of 1·35 was calculated to normalize the soma area values.

Patch-clamp recordings

Intracellular recordings were obtained from isolated LGN neurones using the whole-cell version of the patch-clamp technique (Hamill *et al.* 1981). Patch pipettes were fabricated from borosilicate glass (1BBL, 1·5; World Precision Instruments, Sarasota, FL, USA) and were connected to an EPC-7 amplifier (List Medical Systems, Darmstadt, Germany). Typical electrode resistance was 3–5 MΩ in the bath, with access resistance in the range of 4–8 MΩ. Series resistance compensation > 50% was routinely used. Current records were low-pass filtered at 3 kHz (3-pole Bessel filter). Voltage-clamp experiments were governed by pCLAMP software, operating via a LabMaster DMA interface (Model TL-1-125; both from Axon Instruments, Foster City, CA, USA) on an IBM AT computer. To remove interference from linear leak and capacitive currents, a P/5 pulse protocol was used, in which the currents elicited by each voltage pulse were added to those produced by consecutive steps of one-fifth of the size and of opposite polarity. Current-clamp recordings were digitized (NeuroCorder DR-390; Neurodata, New York, NY, USA) and stored on videotape for later analysis.

Extra- and intracellular solutions

Experiments were conducted at room temperature. Oxygenated, extracellular solution was continuously perfused (0·1–1 ml min^{-1}) through the recording chamber. A multi-barrelled, laminar flow perfusion system was installed close to the recorded neurone, which allowed a rapid exchange (< 1 s) of solutions at a relatively low flow rate (0·1 ml min^{-1}). The basic extracellular solution contained (mM): KCl, 1; dextrose, 10, D-mannitol, 10, *N*-(2-hydroxyethyl)piperazine-*N*′-2-ethanesulphonic acid (Hepes), 10; pH = 7·35. The basic intracellular solution in the patch pipette contained (mM): NaCl, 10; $MgCl_2$, 2; $CaCl_2$, 1; ethyleneglycol-bis-(β-aminoethyl ether)-*N*,*N*,*N*′,*N*′-tetraacetic acid (EGTA), 11; Na_2ATP, 5; Na_2GTP, 0·5; pH = 7·35. The basic solutions had a number substances added to them.

Solutions 1. To maximize/characterize membrane K^+ currents the following additions were made to the basic extracellular solution: NaCl, 135 mM; $CaCl_2$, 1 mM; $MgCl_2$, 2 mM; tetrodotoxin (TTX), 1·5 μM; tetraethylammonium chloride (TEA), 2–20 mM, as required; 4-aminopyridine

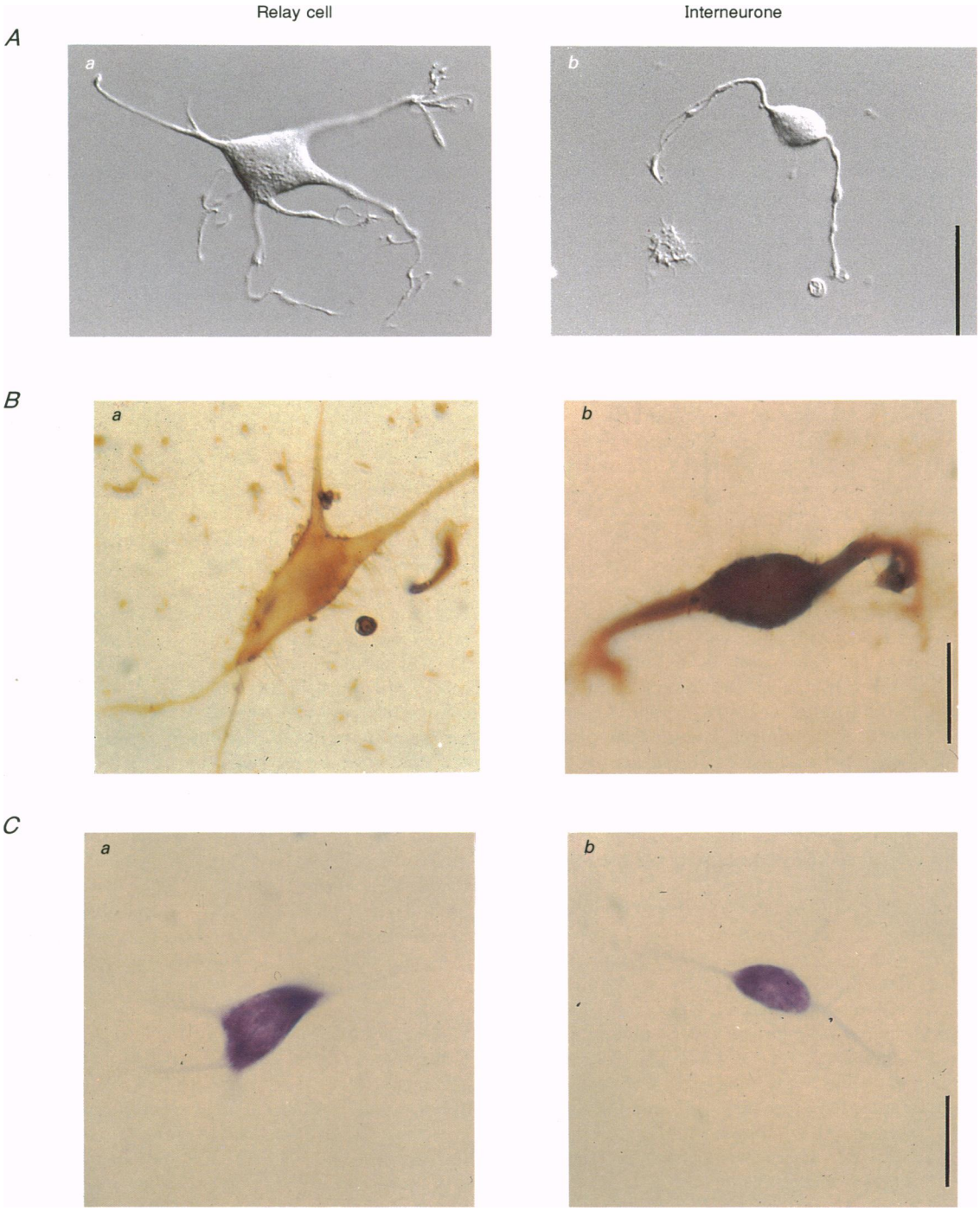

Figure 1. Morphological and immunohistochemical properties of isolated rat LGN neurones
Isolated LGN neurones after acute dissociation (*A*), after immunohistochemical reaction for the presence of GABA (*B*), and after Nissl staining (*C*). Note the two morphological cell types, and the positive reaction for the presence of GABA only in neurones of the small, bipolar type (interneurones, right column), and not in neurones of the large, multipolar type (relay cells, left column). Scale bar indicates 20 μm in *A*, and 10 μm in *B* and *C*.

(4-AP), 2–8 mM, as required. The intracellular solution was modified by the addition of 128 mM KCl.

Solutions 2. To isolate/maximize membrane Ca^{2+} currents the following substances were added to the extracellular solution: NaCl, 120 mM; $CaCl_2$, 2 mM; $MgCl_2$, 1 mM; TTX 1·5 μM; TEA, 20 mM; 4-AP, 6 mM. The intracellular solution was modified by the addition of 128 mM *N*-methyl-D-glucamine and 20 mM TEA.

Solutions 3. To evaluate functional interactions of I_T and I_A in single neurones the following substances were added to the extracellular solution: NaCl, 120 mM; $CaCl_2$, 2 mM; $MgCl_2$, 1 mM; TTX, 1·5 μM; TEA, 20 mM; 4-AP, 6 mM, as required. The intracellular solution was modified by the addition of 128 mM KCl.

Solutions 4. To assess neuronal firing properties under current-clamp conditions the following substances were added to the extracellular solution: NaCl, 135 mM; $CaCl_2$, 2 mM; $MgCl_2$, 1 mM; 4-AP, 6 mM, as required. The intracellular solution was modified by the addition of 128 mM KCl.

Analysis of data

Inactivation and activation curves were obtained from the amplitude of the membrane current (I) that was normalized with respect to the maximal current amplitude (I_{max}) and plotted against the membrane potential (V). The data points were fitted to a Boltzmann function of the form:

$$I/I_{max} = (1 + \exp((V - V_h)/k))^{-1}, \quad (1)$$

where V_h is the potential of half-(in)activation and k is the slope factor indicating the steepness of the calculated curve. Equation (1) applies both to inactivation and activation curves, the slope factor assuming a positive and negative value, respectively. For activation and inactivation curves of membrane K^+ conductances, the conductance g was estimated from the amplitude I of the membrane current as $g = I/(V - E_K)$, with E_K representing the value of the K^+ equilibrium potential, and was normalized with respect to the maximal conductance g_{max}.

The time course of decay of the membrane current was approximated to exponential functions of the form:

$$I = A_0 + A_1\exp(-t/\tau_1) + A_2\exp(-t/\tau_2) + \ldots, \quad (2)$$

where A_0 to A_n are the amplitude coefficients and τ_1 to τ_n are the time constants. Equation (2) was also used to describe the time course of recovery from inactivation of a membrane current that was normalized with respect to the maximal current amplitude (I/I_{max}).

Data are presented as means ± S.D. and number of observations (n). Paired samples were statistically analysed using Student's two-tailed t test.

RESULTS

Identification of local circuit neurones and relay cells

In the rat LGN the two major neuronal types, local circuit neurones and cortically projecting relay neurones, possess distinctive morphological and immunohistochemical properties, and these distinguishing features were largely retained in neurones that were isolated from the surrounding tissue (see Discussion). In a population of acutely dissociated rat LGN cells, neurones possessing a multipolar cell body (14–25 μm in diameter) giving rise to three to five bifurcating dendrites (1–3 μm in diameter) extending up to 30 μm from the soma, and smaller neurones (around 10 μm in diameter) of a fusiform or oval shape with processes emerging from opposite poles of the soma were easily distinguishable (Fig. 1*A*). The existence of these morphologically distinctive types of isolated LGN neurones was corroborated through Nissl staining (Fig. 1*C*). In the intact rat LGN, neurones with similarly shaped cell bodies have been shown to represent GABA-negative relay neurones and GABAergic local circuit cells, respectively (Ohara *et al.* 1983; Gabbott *et al.* 1986). Indeed, the LGN neurones could be immunohistochemically identified even after isolation. Acutely dissociated multipolar neurones possessing a large multipolar soma were GABA immunonegative, whereas the small bipolar neurones stained positive for the presence of GABA or the GABA-synthesizing enzyme GAD (Fig. 1*B*). Figure 2 provides quantitative data obtained from the two-dimensional analysis of the soma profiles in a total of 3441 isolated LGN neurones. The size distributions of the somatic areas were significantly different for acutely dissociated multipolar (mean, 214·9 ± 60·7 μm²; $n = 398$) and for bipolar neurones (103·1 ± 29·3 μm²; $n = 84$; Fig. 2*A*). Very similar bimodal size distributions of somatic areas were obtained for isolated GABA/GAD-immunonegative (229·4 ± 100·1 μm²; $n = 1821$) and -immunopositive neurones (97·7 ± 33·3 μm²; $n = 473$; Fig. 2*B*), and for isolated Nissl-stained neurones with multipolar (222·1 ± 60·8 μm²; $n = 537$) and bipolar cell bodies (100·2 ± 30·7 μm²; $n = 128$; Fig. 2*C*). The relative proportion of acutely dissociated bipolar neurones, of isolated GABA/GAD-positive neurones, and of isolated bipolar cells after Nissl staining was 17·4, 20·6 and 19·2%, respectively.

Following from this we conclude that relay cells and local circuit interneurones of the rat LGN can be reliably identified after acute dissociation and therefore we refer to them as such.

Basic firing properties of isolated neurones

In order to compare the basic firing properties of the two classes of neurones after isolation, we performed whole-cell recordings under current-clamp conditions in a limited number of cells ($n = 10$). The membrane resting potential of the cells was in the range −55 to −70 mV, and the injection of a small depolarizing current pulse elicited a tonic series of Na^+–K^+-mediated action potentials in both types of neurones. When the cells were slightly hyperpolarized from rest (e.g. to −76 mV, Fig. 3*A*), the onset to spike firing was typically delayed in multipolar relay cells, probably due to the activation of transient membrane K^+ conductances

(Huguenard & Prince, 1991; McCormick, 1991; Budde *et al.* 1992), whereas we did not observe a delayed onset to firing when depolarizing stimuli were applied to bipolar local circuit neurones. A difference in the duration of single spikes between the two types of neurones could not be reliably determined under the present experimental conditions. Following hyperpolarizing membrane deflections, multipolar cells generated the Ca^{2+}-mediated action potential with a low threshold of activation triggering one to two fast spikes (Fig. 3*B*) characteristic of thalamocortical relay neurones (Jahnsen & Llinás, 1984*a*, *b*; Steriade & Deschênes, 1984). By contrast, local circuit neurones completely lacked this type of Ca^{2+}-mediated response (Fig. 3*B*), or they generated a small depolarizing 'hump' upon termination of large membrane hyperpolarizations (Fig. 11*B*).

These differences in basic firing properties are typical of those previously described for relay cells and local circuit interneurones that were morphologically identified in the slice preparation of the cat LGN (McCormick & Pape, 1988; McCormick, Pape, Kisvárday & Eysel, 1992), and they confirm our conclusion that the results presented here reflect the intrinsic properties of these two classes of geniculate neurones.

Properties of Ca^{2+} currents

In a first approximation, the differences in the low-threshold Ca^{2+} response between LGN relay cells and interneurones could be due to differences in the underlying

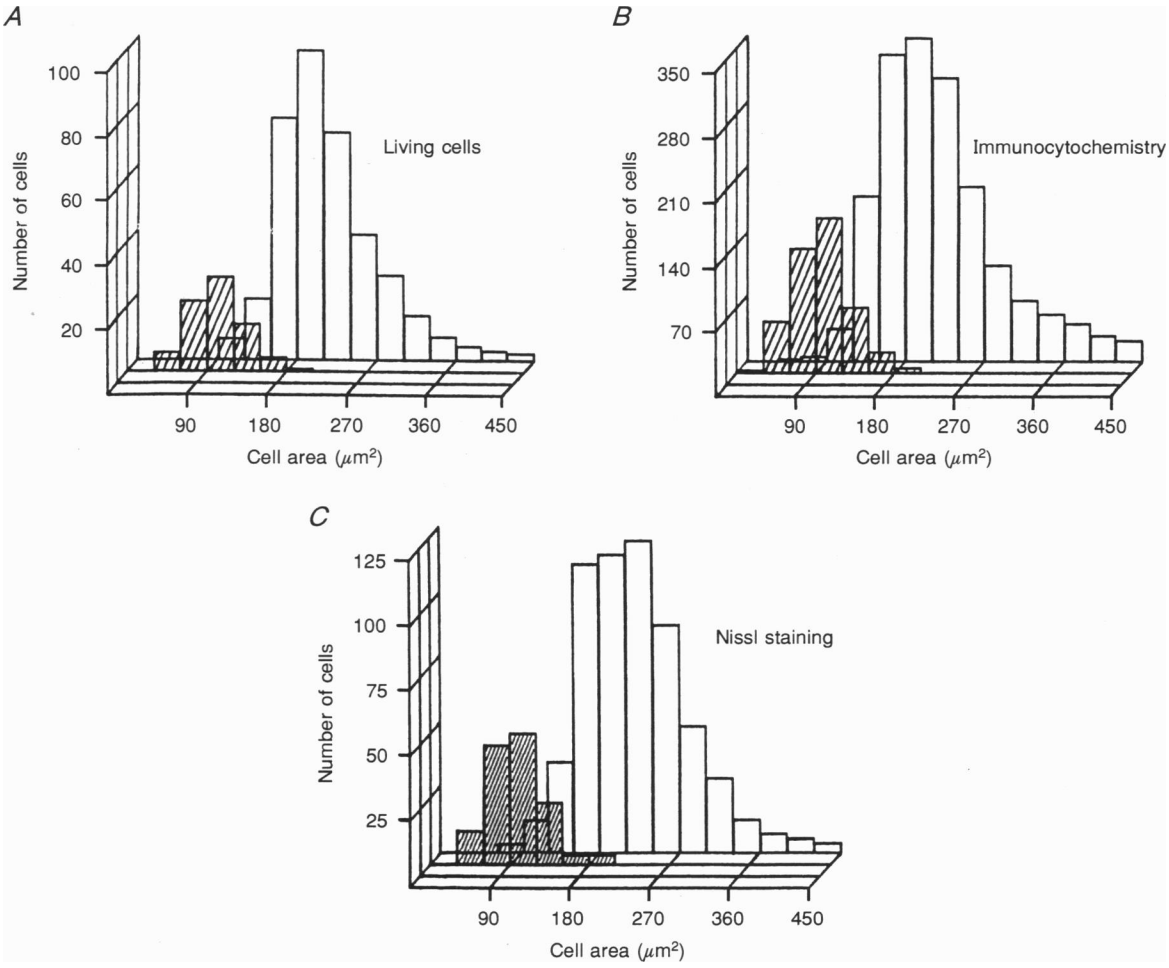

Figure 2. Size–frequency distributions of soma areas in three populations of isolated LGN neurones

A, 'living' cells after acute dissociation; *B*, cells after immunohistochemical reaction for the presence of GABA or GAD; and *C*, cells after Nissl staining. Cell populations were divided into two groups according to the soma profile ('multipolar', □; 'bipolar', ▨; *A* and *C*) or the immunonegative (□)/immunopositive (▨) reaction for the presence of GABA or GAD (*B*). Histograms are obtained from the two-dimensional analysis of the somatic surface area. The ordinate represents the number of cells within each 30 μm^2 size class along the abscissa. Note the very similar bimodal size distributions for all three populations of LGN neurones, with small bipolar, GABA-positive neurones representing about 20% of the total neuronal population. See text for statistical data on these distributions.

T-type Ca^{2+} channels. We evaluated this hypothesis by performing whole-cell voltage-clamp experiments in acutely dissociated neurones under conditions in which membrane Ca^{2+} currents were isolated. Specifically, K^+ ions in the patch pipette were substituted by *N*-methyl-D-glucamine and TEA was added; the extracellular medium contained TEA, 4-AP and TTX (see Methods). Under these conditions, depolarization of the membrane in the range between −80 and −40 mV from a holding potential of −110 mV evoked transient inward currents whose amplitudes increased with more positive values of the membrane potential (Fig. 4*A*). The inward currents were carried by Ca^{2+} ions, as indicated by their sensitivity toward changes in the extracellular Ca^{2+} concentration and their blockade by 50 μM nickel (Ni^{2+}, data not shown; cf. Hernández-Cruz & Pape, 1989).

The basic features of these Ca^{2+} currents were similar in relay cells and local circuit interneurones. From a holding potential of −110 mV, the currents were rapidly activated through depolarizing voltage steps. The time to peak decreased with more positive values of the membrane potential, ranging between 18·1 ± 5·5 and 6·9 ± 2·0 ms in relay cells ($n = 13$), and between 21·9 ± 5·4 and 7·2 ± 1·4 ms in interneurones ($n = 11$), in the range of membrane voltage between −65 and −40 mV (Fig. 4*D*). The Ca^{2+} currents inactivated completely with maintained depolarization, and they could not be elicited from holding potentials positive to −50 mV. The time course of decay of inward current was well described by a single exponential function (eqn (2)). The inactivation time constants exhibited moderate voltage dependence and ranged from 31·9 ± 12·1 to 19·8 ± 3·6 ms in relay cells ($n = 12$), and from 40·0 ± 11·4 to 20·2 ± 3·9 ms in interneurones ($n = 11$), in the voltage range between −65 and −40 mV (Fig. 4*B* and *C*). The transient inward current in local circuit neurones, which had very similar behaviour to the T-type Ca^{2+} current in isolated LGN relay cells (cf. Hernández-Cruz & Pape, 1989), decreased in size after equimolar substitution of extracellular Ca^{2+} by barium ions (Ba^{2+}), and was readily blocked by addition of 50 μM Ni^{2+} to the bathing medium (data not shown). Although we observed a typical T-type Ca^{2+} current in more than 80% of our sample of interneurones ($n = 34$), it was significantly smaller in size (mean maximal amplitude, 109 ± 46 pA; $n = 11$) than that in relay cells (289 ± 131 pA; $n = 16$), and the steady-state voltage dependence of I_T was different in the two types of LGN neurones. Figure 5 illustrates experiments in which activation and inactivation properties of I_T were analysed more quantitatively. From a holding potential of −110 mV, the membrane potential was stepped in +5 mV increments

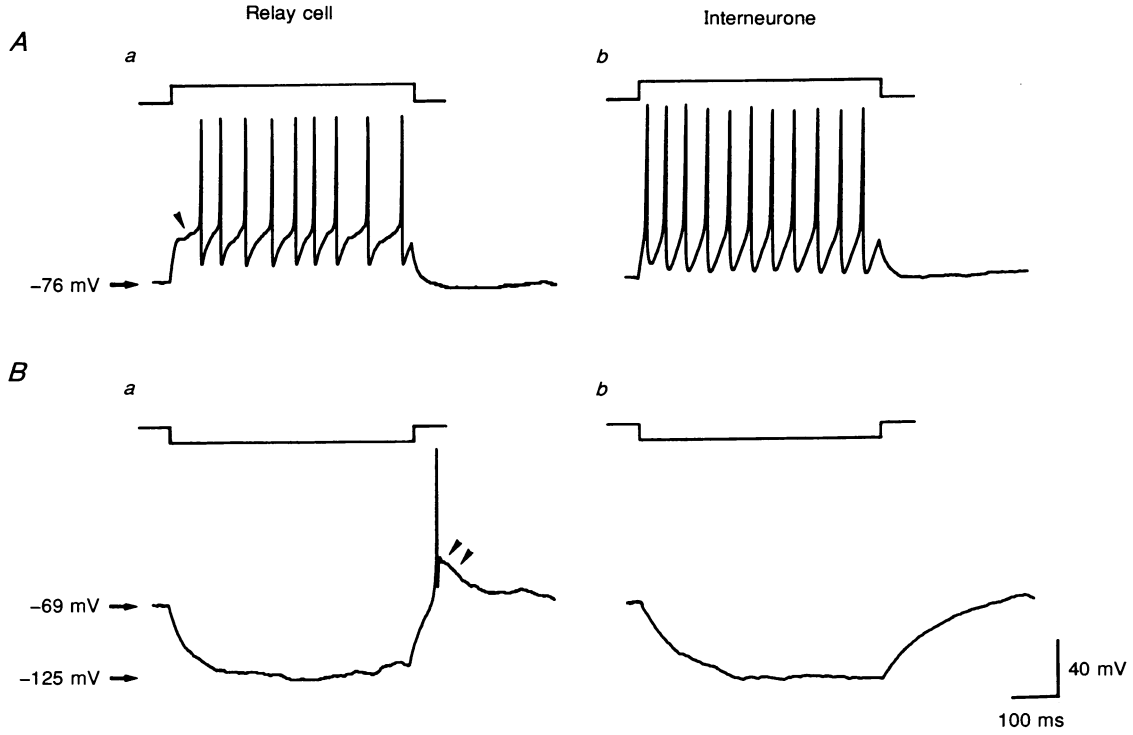

Figure 3. Basic firing properties of a relay cell (left column) and an interneurone (right column) acutely dissociated from the rat LGN

A, a depolarizing current pulse induces a tonic series of fast action potentials in both types of neurones, and is characteristically delayed in onset in the relay cell (arrowhead in *a*), not in the interneurone (*b*). *B*, the break of a hyperpolarizing current pulse evokes a slow regenerative rebound response triggering a fast action potential in the relay cell (double arrowhead in *a*), not in the interneurone (*b*). Initial and steady-state values of the membrane potential as indicated.

(Fig. 5C). The normalized peak amplitudes of the evoked currents were averaged, plotted against the step depolarization, and a Boltzmann function (eqn (1)) was approximated to the data points. The activation curves of I_T in the two types of LGN neurones were clearly separated on the voltage axis (filled and open circles in Fig. 5B). Threshold (at around −70 mV) and half-activation of I_T in local circuit neurones (−54·9 ± 4·7 mV; $n = 11$) occurred at significantly ($P < 0·01$) more positive values of the membrane potential than in relay neurones (threshold at −80 mV; half-activation at −64·5 ± 7·0 mV; $n = 17$), whereas the steepness of the activation curve was not significantly different in the two classes of cells ($k = -4·8 \pm 1·5$ *vs.* $-4·9 \pm 0·9$ mV^{-1}).

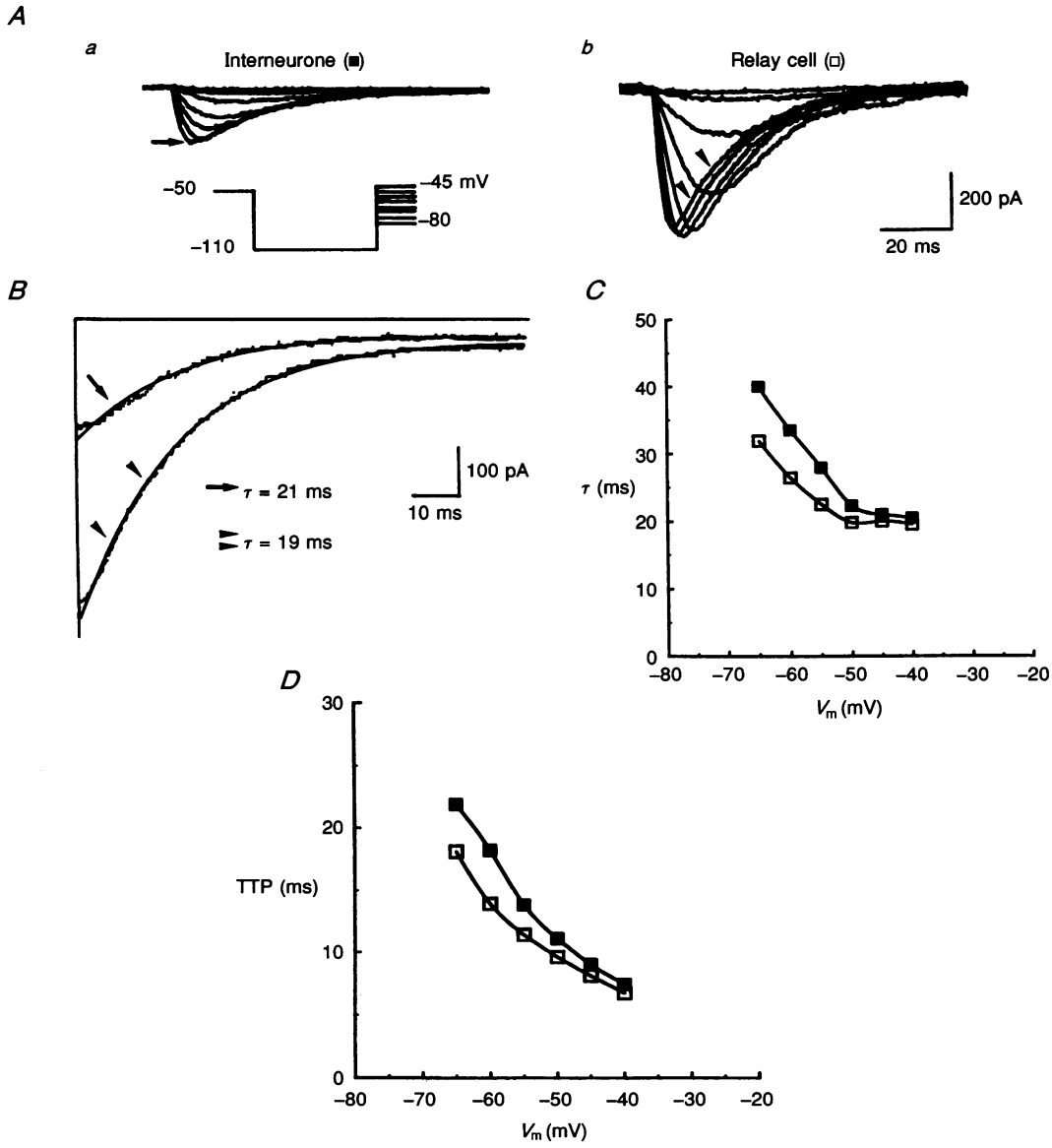

Figure 4. Activation and decay of the T-type Ca^{2+} inward current in LGN interneurones and relay cells

A, transient Ca^{2+} inward currents with increasing amplitude evoked in an interneurone (*a*) and a relay cell (*b*) by 5 mV increments in test potentials in the range −80 to −45 mV, following a hyperpolarizing prepulse of 1 s duration to −110 mV (pulse protocol as indicated). *B*, examples from experiment in *A* of current decay during a sustained voltage step to −45 mV, in the interneurone (arrow) and the relay cell (double arrowhead). The smooth curves represent the best fit of a monoexponential function (eqn (2)) through the data points. Time constants of inactivation of the inward current are 21 and 19 ms in the two types of neurones. Plotting the time constants of I_T decay (*C*) and the time to peak (TTP) of I_T (*D*) as functions of the step potential indicates moderately voltage-dependent kinetic properties of I_T in the two types of cells. Data were averaged from a larger sample of interneurones (■) and relay cells (□); differences are not significant. Standard deviations of the mean have been omitted from the plots for clarity; see text for statistical data.

The positive shift in the activation curve of I_T in interneurones was paralleled by a shift in the steady-state inactivation properties of I_T to more positive values of the membrane potential. Figure 5*A* illustrates the pulse protocol and a sample of current records used to construct the steady-state inactivation curve. A prepulse of 1 s duration was altered between −110 and −65 mV in +5 mV increments, and a constant test pulse to −40 mV was applied to near maximally activate I_T. The normalized peak amplitudes of the currents were averaged and plotted against the prepotential. Approximation of a Boltzmann function (eqn (1)) to the data points indicated the range of steady-state inactivation of I_T in the two types of cells (filled and open squares in Fig. 5*B*), with a significantly ($P < 0.05$) different value of half-inactivation in interneurones ($V_h = -81.1 \pm 5.1$ mV, $k = 4.6 \pm 1.1$ mV^{-1}; $n = 11$) and in relay cells ($V_h = -86.1 \pm 5.8$ mV, $k = 4.9 \pm 1.0$ mV^{-1}; $n = 30$).

Although the activation curve, constructed from peak current values rather than from the amplitude of tail currents, disregards driving force and inactivation and as such is a crude representation of the voltage-dependent activation process of I_T, values near the threshold are expected to be more accurate than those at more positive potentials. Thus, the values of 50% activation of I_T calculated from peak current values were not significantly different from those calculated from initial amplitudes of I_T at the onset of the depolarizing pulse (as extrapolated from the exponential decay of I_T). In addition, the relative difference in the change in Ca^{2+} conductance as a function of voltage between the two types of cells can be assumed to be sufficiently well indicated.

The low-threshold Ca^{2+}-mediated action potential in thalamocortical relay neurones demonstrates refractoriness to generation of the second response (Jahnsen & Llinás, 1984*a*,*b*), due to a slow process of recovery from inactivation of I_T (Coulter *et al.* 1989; Crunelli *et al.* 1989; Hernández-Cruz & Pape, 1989). We compared the removal of inactivation of I_T in interneurones with that in relay cells using the voltage pulse protocol illustrated in Fig. 6. The current was inactivated by a holding potential of −50 mV, and inactivation was increasingly removed by hyperpolarization of the membrane to −110 mV for an increasing period of time, before a final step to −45 mV activated I_T. In Fig. 6*C*, the normalized peak currents in local circuit neurones (open circles) and relay cells (filled circles) are plotted as a function of prepulse duration. The time course of recovery from inactivation of I_T was approximated best by a single exponential function, and the mean time constants were very similar in both types of neurones (218·1 ± 26·1 ms in 5 interneurones; 205·9 ± 51·9 ms in 6 relay cells).

In conclusion, the GABAergic local circuit neurone of the rat LGN possesses a transient Ca^{2+} current with

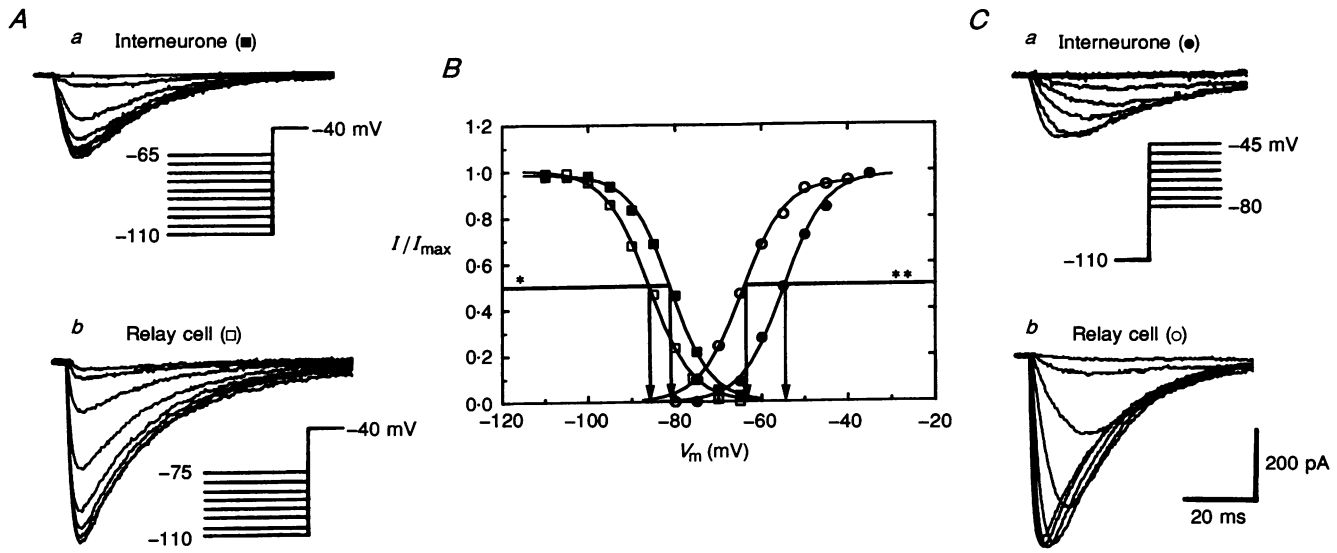

Figure 5. Characteristics of steady-state inactivation and activation of I_T in relay cells and interneurones

A, inactivation of I_T was determined by varying a prepulse of 1 s duration between −110 mV and −65 mV, keeping the test potential at −40 mV to activate I_T. Examples of currents are shown for an interneurone in *a* and for a relay cell in *b*. *C*, activation of I_T was measured by applying depolarizing voltage steps from −110 mV to various test potentials in the range between −80 and −45 mV. Examples of currents for an interneurone in *a* and for a relay cell in *b*. *B*, inactivation curves (interneurones: ■, $n = 11$; relay cells: □, $n = 30$) and activation curves (interneurones: ●, $n = 11$; relay cells: ○, $n = 17$) were obtained by fitting a Boltzmann function (eqn (1)) to plots of the mean values of the normalized peak current against the test potential and the prepulse potential, respectively. The differences observed between the two types of neurones in half-maximal activation and inactivation of I_T are significant (**$P < 0.01$ and *$P < 0.05$, respectively). Standard deviations of the mean have been omitted for clarity; see text for further statistical data.

properties characteristic of the T-type Ca^{2+} current, but a steady-state voltage dependence which is positively shifted by about +10 mV compared with that in relay cells. Although the maximal amplitude of the whole-cell current is substantially smaller in size in local circuit neurones than that in relay neurones, the mean size of I_T is very similar in the two types of LGN cells when the difference in membrane surface area between the two types of cells (see above) is taken into account (1·1 pA μm^{-2} in interneurones, and 1·3 pA μm^{-2} in relay cells). Very interestingly, interneurones were also found to possess a non-inactivating, L-type Ca^{2+} current very similar to that of relay cells (cf. Hernández-Cruz & Pape, 1989), which (i) was activated through depolarization positive to −35 mV, (ii) could be elicited in isolation from holding potentials positive to −50 mV, (iii) was readily abolished by 50 μM cadmium in the bathing medium, and (iv) was increased in size with Ba^{2+} as the charge carrier (data not shown).

Properties of the A-type K^+ current

The presence in local circuit cells of a characteristic T-type Ca^{2+} current with merely quantitative differences in the range of activation/inactivation compared with those in relay cells was not sufficient to account for the general absence and presence of the Ca^{2+}-mediated action potential observed in the two types of LGN neurones. One intrinsic cellular mechanism that can be expected to functionally interact with the Ca^{2+} current is the activation of an opposing K^+ current, which may slow or even prevent the generation of the Ca^{2+} action potential. Among the distinct K^+ conductances inherent to thalamocortical relay neurones (Huguenard & Prince, 1991; Huguenard, Coulter & Prince, 1991; McCormick, 1991; Budde *et al.* 1992), the fast transient A-type current (I_A) operates in a range of membrane voltages and possesses kinetic properties partly overlapping with those of the T-type Ca^{2+} current, probably allowing for interactions in relation to shaping the low-threshold Ca^{2+} response. Therefore, experimental steps were designed to search for a respective K^+ conductance in local circuit neurones, to quantitatively analyse its properties, and to compare it with that in relay cells. Under whole-cell voltage-clamp conditions that maximized membrane K^+ currents (solutions 1, as specified in Methods), small depolarizing steps from negative holding potentials (e.g. −90 mV) evoked a fast transient K^+ current in interneurones, whose amplitude increased rapidly with increasing depolarization (Fig. 7*A*). The current inactivated completely within 60–80 ms during the

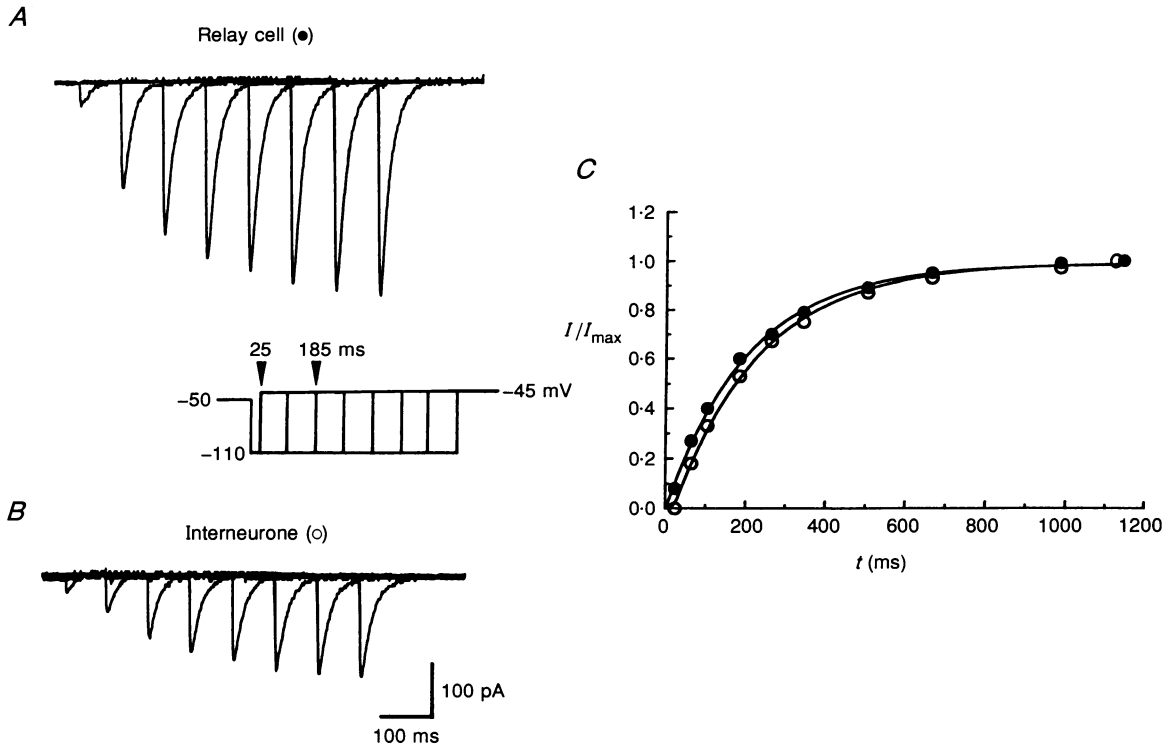

Figure 6. Recovery from inactivation of I_T in the two types of LGN cells
A relay cell (*A*) and an interneurone (*B*) were held at −50 mV to completely inactivate I_T, and hyperpolarizing steps of varying duration to −110 mV were applied, followed by a step to −45 mV to activate I_T. *C*, the normalized amplitudes of I_T, averaged from a larger sample of interneurones (○, $n = 5$) and relay cells (●, $n = 6$) are plotted against the prepulse duration (t); the continuous lines represent monoexponential fits (eqn (2)) to the data points. The time constants of recovery from inactivation of I_T were not significantly different in interneurones (218·1 ± 26·1 ms) and relay cells (205·9 ± 51·9 ms).

depolarizing step, and it could not be elicited from holding potentials positive to −50 mV. With larger depolarizing voltage steps (i.e. positive to −30 mV), additional slower declining components of outward current were elicited. The fast kinetics of activation and inactivation of the fast transient K^+ current were indicative of the A-type K^+ conductance, which was corroborated by its pharmacological profile, i.e. relative insensitivity to extracellularly applied TEA (up to 20 mM) and blockade by 2–8 mM 4-AP.

In the following experiments, the properties of I_A were studied in the presence of TEA (10–20 mM), which minimized contamination by the slowly decaying components of K^+ conductance. I_A was separated from the remaining current by addition of 4-AP (6 mM) to the perfusate or by leaving a conditioning pulse of 75–100 ms duration to −40 mV between a hyperpolarizing prepulse to −110 mV and the depolarizing test pulse (cf. Budde *et al.* 1992). These protocols eliminated I_A, and the subtraction currents obtained from records either before and during the presence of 4-AP or from records without and with the conditioning pulse showed I_A in isolation (examples in Figs 7 and 8). In both types of LGN neurones, the current peaked within 1–5 ms and declined completely during the depolarizing pulse (Fig. 7*A*). Significant differences were observed in the time course of decay. In interneurones, inactivation was terminated about 80 ms after onset of the depolarizing pulse. The time course of inactivation was described best by a monoexponential function (Fig. 7*B*; eqn

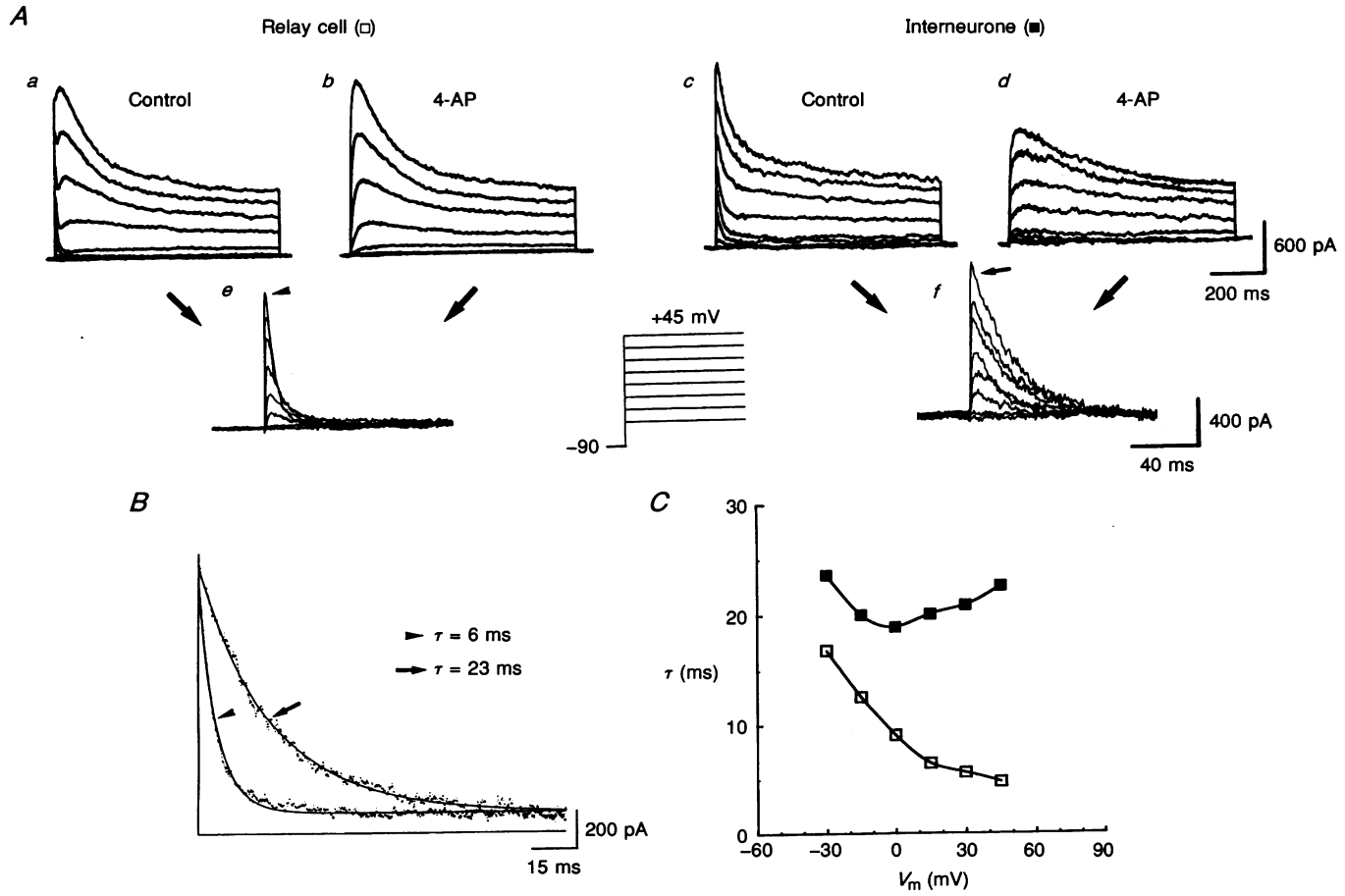

Figure 7. Activation and decay characteristics of the A-type K^+ current in the two types of LGN neurones

A, incrementing depolarizing voltage steps from −90 mV evoked several types of K^+-mediated outward current in a relay cell (*a*) and in an interneurone (*c*), of which components other than I_A were reduced by adding TEA (10 mM) to the bathing medium. The subtraction currents, obtained from records before (*a* and *c*) and during action of 6 mM 4-AP (*b* and *d*), represent I_A, which rapidly activated and completely declined during depolarizing steps in the relay cell (*e*) and in the interneurone (*f*). *B*, examples from subtraction currents in *A* (voltage step to +45 mV) indicate a monoexponential time constant of I_A decay, measuring 6 ms in the relay cell (arrowhead) and 23 ms in the interneurone (arrow). Continuous lines through the data points represent monoexponential fits (eqn (2)). *C*, plots of the time constants of I_A decay as a function of the test potential, averaged from a larger sample of interneurones (■, $n = 16$) and relay cells (□, $n = 19$). Note the fast and voltage-dependent time course of I_A decay in relay cells compared with the slower time constants and no clear dependence on membrane voltage in interneurones. See text for statistical data.

(2)). The time constants displayed no obvious voltage dependence, with means of 23·6 ± 10·9, 18·9 ± 8·0 and 22·5 ± 6·9 ms ($n = 16$) for depolarizations to −30, 0 and +45 mV, respectively (Fig. 7*C*, filled squares). In relay cells, by comparison, the decay of I_A was significantly faster, inactivation was completed in less than 40 ms (Fig. 7*A*), and the time constants of inactivation (Fig. 7*B*) exhibited voltage dependence ranging from 16·8 ± 6·6 to 4·7 ± 2·1 ms ($n = 19$) between −30 and +45 mV (Fig. 7*C*, open squares). Further differences were found in the voltage-dependent properties of I_A between the two types of neurones; typical experiments are illustrated in Fig. 8. The activation properties of I_A were investigated using the subtraction currents of the 4-AP or prepulse experimental protocols (examples of current traces in Fig. 8*C*). The normalized peak conductances of I_A plotted against the step depolarization were well described by a Boltzmann function (eqn (1)). In local circuit neurones, the activation curve of I_A was shifted to more negative values on the voltage axis (filled circles in Fig. 8*B*); half-activation occurred at significantly ($P < 0·0001$) more negative values ($V_h = -25·2 \pm 7·0$ mV; $n = 22$) than in relay cells ($V_h = -14·5 \pm 6·9$ mV; $n = 22$; open circles in Fig. 8*B*), whereas the slope of the curves was not significantly different ($k = -12·4 \pm 3·2$ mV^{-1} and $-14·3 \pm 3·2$ mV^{-1}, respectively). The steady-state inactivation characteristics of I_A were determined by varying a 1 s prepulse between −110 and −35 mV. External TEA (20 mM) was present to eliminate the more slowly decaying components of outward current. A test pulse to −10 mV was chosen to minimize contamination by the TEA-insensitive component of the inactivating K^+ conductance (I_{Km}) present in LGN relay cells, which is only about 20% activated at this potential (cf. Budde *et al.* 1992). Normalized peak conductances from current ensembles shown in Fig. 8*A* were plotted against the prepotential. Approximation of a Boltzmann function (eqn (1)) to the data points yielded a significant difference in the range of inactivation of I_A in the two classes of cells (Fig. 8*B*, filled and open squares), indicated by the significantly more negative value of half-inactivation in local circuit neurones (−82·8 ± 8·3 mV; $n = 17$) compared with that of relay cells (−69·2 ± 5·6 mV; $n = 21$), and the similar steepness of the curves ($k = 8·3 \pm 2·2$ *vs.* $7·0 \pm 3·7$ mV^{-1}). Finally, we investigated the availability of I_A at different times following membrane depolarization. The current was inactivated by a holding potential of −50 mV, and a prepulse to −110 mV was applied for periods between 2·5 and 500 ms before a final pulse to −10 mV activated I_A. Examples of current traces in relay cells and interneurones are shown in Fig. 9*A* and *B*, respectively. The normalized

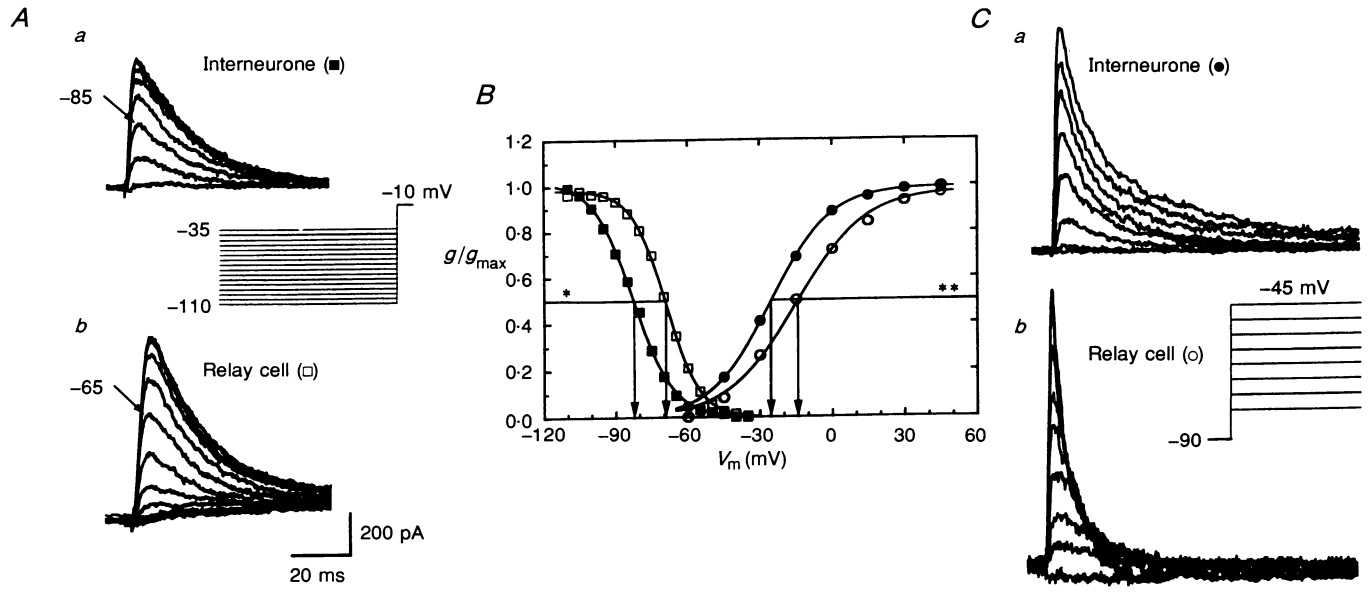

Figure 8. Steady-state voltage-dependent properties of I_A

Experimental isolation of I_A through the use of 4-AP or a conditioning prepulse of 75–100 ms duration to −40 mV (see text). *A*, inactivation was determined by varying a 1 s prepulse between −110 and −35 mV, and keeping the following test potential at −10 mV. Examples of I_A in an interneurone (*a*) and a relay cell (*b*). *C*, activation of I_A, as measured through depolarizing steps of increasing amplitude from a holding potential of −90 mV. Examples in an interneurone (*a*) and a relay cell (*b*). *B*, inactivation curves (interneurones: ■, $n = 22$; relay cells: □, $n = 22$) and activation curves (interneurones: ●, $n = 17$; relay cells: ○, $n = 21$) obtained through Boltzmann fits (eqn (1)) demonstrate significant differences between the two types of cells in the range of I_A activation (*$P < 0·0001$) and of I_A inactivation (**$P < 0·0001$). See text for more detailed statistical data. Experiments were performed during the presence of external TEA (20 mM).

peak currents were averaged and plotted against prepulse duration. Approximation of a monoexponential function (eqn (2)) to the data points indicated a significantly ($P < 0{\cdot}02$) slower time course of recovery from inactivation of I_A in interneurones ($\tau = 76{\cdot}9 \pm 35{\cdot}8$ ms; $n = 5$) compared with that in relay cells ($\tau = 21{\cdot}1 \pm 5{\cdot}3$ ms; $n = 8$).

In conclusion, local circuit neurones and relay cells in the rat LGN possess a voltage-dependent membrane K^+ current (I_A), whose kinetic and voltage-dependent properties resemble those of the T-type Ca^{2+} current. While the maximal K^+ conductance is similar in interneurones ($7{\cdot}6 \pm 2{\cdot}6$ nS; $n = 15$) and in relay cells ($10{\cdot}9 \pm 3{\cdot}8$ nS; $n = 16$), the range of activation and inactivation of I_A is negatively shifted by about −10 mV in interneurones compared with that in relay cells, and the process of inactivation (and removal from inactivation) of I_A takes significantly longer to be completed in interneurones than in relay cells. When the difference in membrane surface area between the two types of cells is taken into account (see above), the maximal A-conductance is slightly ($P < 0{\cdot}01$) higher in interneurones (9·6 pS μm^{-2}) compared with that in relay cells (8·0 pS μm^{-2}).

Interactions between I_T and I_A

The voltage-clamp analysis revealed many similarities between I_A and I_T in terms of their time courses and voltage dependencies. There are, however, quantitative differences in amplitude and steady-state voltage-dependent properties of the two opposing membrane currents in the two classes of LGN neurones, presumably resulting in distinct functional interactions in the two types of cells (see Discussion). One prominent parameter in shaping the interactions between I_A and I_T relates to their threshold of activation. In Fig. 10*A*, current *versus* voltage (I–V) relationships of I_A and I_T were constructed from averaged peak currents activated by depolarizing pulses from −110 mV under conditions that maximized K^+ and Ca^{2+} currents, respectively (solutions 1 and 2, as described in Methods). In local circuit neurones, both I_T and I_A activated at around −70 mV and rapidly increased in size with further depolarization. In relay cells, by comparison, I_T activated at more negative membrane voltages (threshold at around −80 mV), whereas I_A required a membrane potential positive to −60 mV for activation.

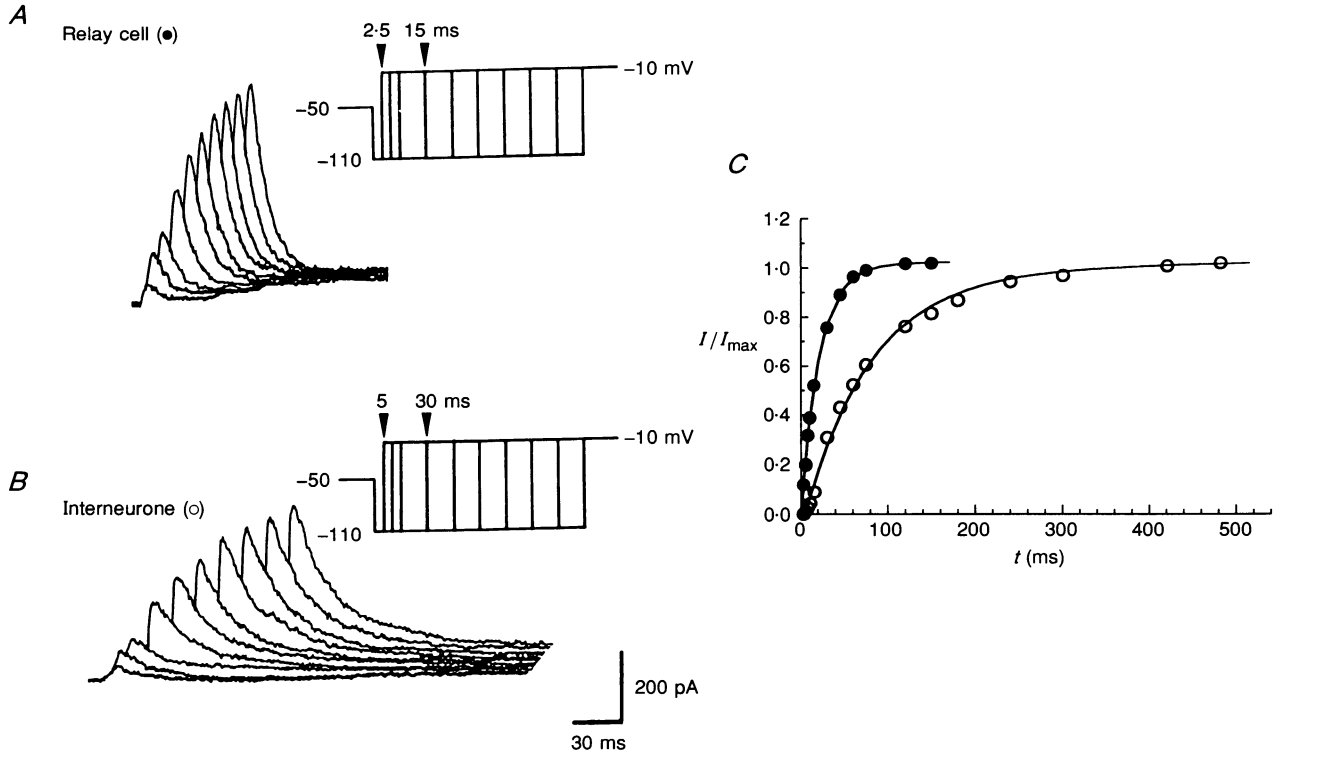

Figure 9. Time course of recovery from I_A inactivation
The holding potential was set to −50 mV, hyperpolarizing prepulses to −110 mV were varied in duration, and a final step to −10 mV activated I_A in a relay cell (*A*) and in an interneurone (*B*). *C*, plots of the normalized amplitudes of I_A as a function of prepulse duration demonstrate a significantly slower time course of recovery from I_A inactivation in interneurones (○; $\tau = 76{\cdot}9 \pm 35{\cdot}8$ ms, $n = 5$) compared with that in relay cells (●; $\tau = 21{\cdot}1 \pm 5{\cdot}3$ ms, $n = 8$). Standard deviations have been omitted from the plots for clarity.

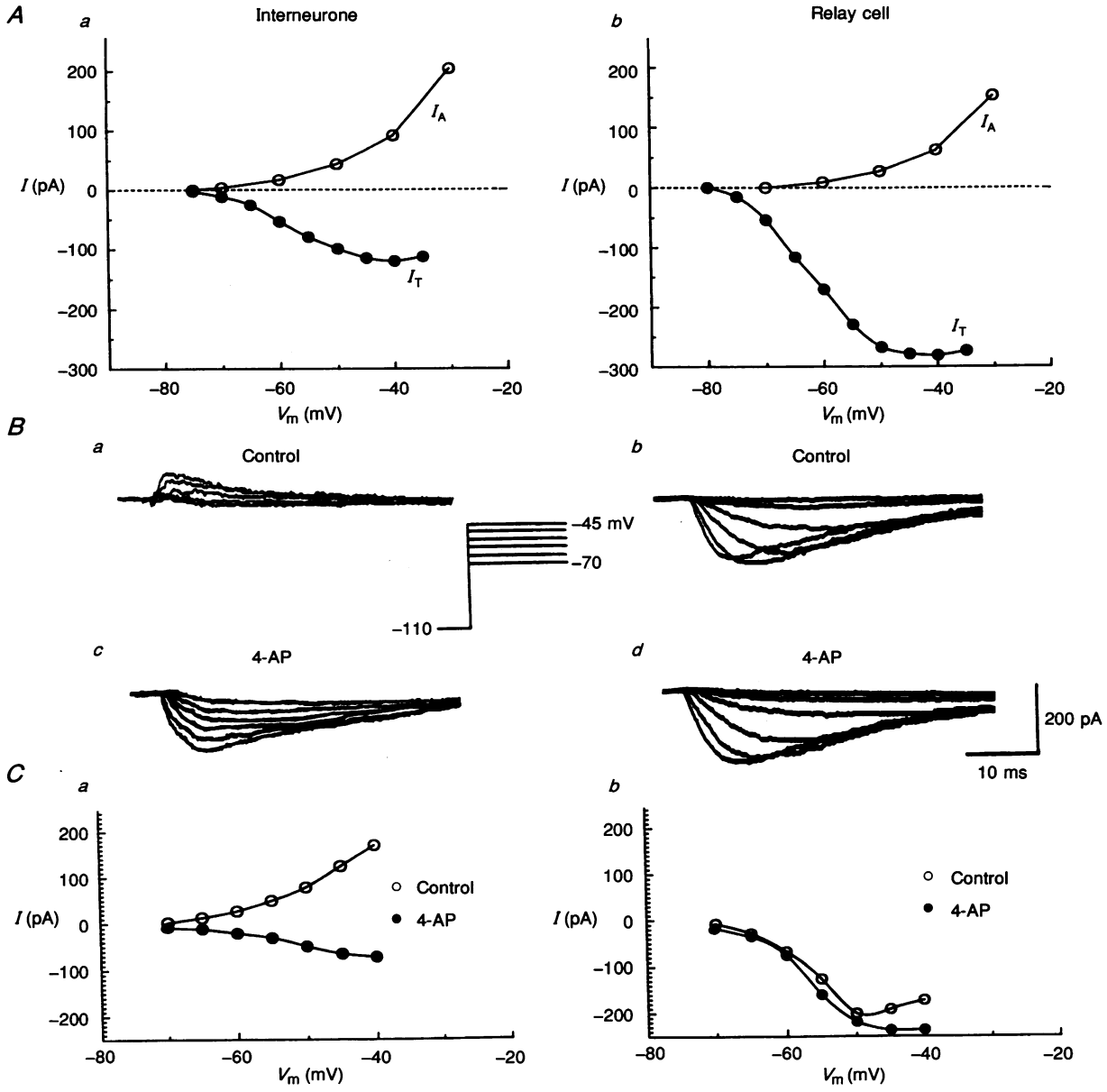

Figure 10. Interactions between I_A and I_T in interneurones and relay cells

A, *I–V* relationships of I_A (○; recorded under conditions that maximize K^+ currents (solutions 1)) and I_T (●; recorded under conditions that isolate Ca^{2+} currents (solutions 2)) averaged from a sample of interneurones (*a*: I_A, $n = 21$; I_T, $n = 16$) and relay cells (*b*: I_A, $n = 19$; I_T, $n = 17$). Recordings were obtained during presence of external TEA (20 mM). Note in interneurones the similar threshold of activation of the two opposing currents (at −70 mV), and in relay cells the activation threshold of I_T at values of the membrane potential (−80 mV) negative to that of I_A (around −65 mV). *B*, net membrane currents obtained in an interneurone and in a relay cell, under whole-cell conditions that allow the flow of K^+ and Ca^{2+} ions across the membrane (solutions 3). During the presence of external TEA (20 mM), depolarization of the membrane to values between −70 and −45 mV from a holding potential of −110 mV (pulse protocol as indicated) induces small transient outward currents in the interneurone (*a*), and voltage-dependent transient inward currents in the relay cell (*b*). With the addition of 6 mM 4-AP to the bathing solution, the same pulse protocol now produces transient voltage-dependent inward currents in the interneurone (*c*) and the relay cell (*d*). *C*, *I–V* relationships from experiments in *B*, obtained from a larger sample of interneurones ($n = 5$) and relay cells ($n = 7$). Plots represent mean values of peak current amplitudes obtained before (Control; ○) and during the presence of 6 mM 4-AP (●). Note in interneurones the similar *I–V* curves of the net outward current and the net inward current present during 4-AP, which are widely overlapping with those of I_A and I_T (*A a*). In relay cells, the *I–V* curve of the inward current largely coincides with that of I_T (*A b*), and the *I–V* curves before and during the presence of 4-AP diverge positive to −60 mV, i.e. in the range of activation of I_A. All recordings were made during the presence of extracellular TEA (20 mM). Currents are leak subtracted. Standard deviations of the mean have been omitted from the plots in *A* and *C* for clarity.

These differences are also reflected by the activation curves, which demonstrate a more negative range of I_T activation in relay cells than in interneurones, whereas the activation range of I_A is positively shifted in relay cells compared with that in local circuit neurones (see Figs 5 and 8).

Following from this, the two membrane currents are expected to interact differentially and thereby to influence differentially the electrical activity in the two types of LGN neurones. We tested this hypothesis by directly comparing the interactions of I_A and I_T in single neurones, using a pharmacological approach. Under whole-cell conditions that allowed the flow of Ca^{2+} and K^+ ions across the membrane (solutions 3; see Methods), TEA (20 mM) was added to the bathing medium, the neurones were held at −110 mV, and depolarizing pulses were applied at levels within the range of activation of I_A and I_T (to between −70 and −40 mV). Using this experimental protocol, the contribution of the more slowly inactivating TEA-insensitive components of K^+ conductance and the L-type Ca^{2+} current can be assumed to be small, since they are less than 10% activated at these potentials (Hernández-Cruz & Pape, 1989; Huguenard & Prince, 1991; Budde *et al.* 1992). The responses to membrane depolarization were completely different in the two types of neurones: relay cells produced a voltage-dependent inward current, I_T, whereas in local circuit cells, a small transient outward current with properties resembling I_A was elicited (Fig. 10*B*, upper traces). Addition of 4-AP (6 mM) to the perfusion medium blocked I_A and thereby unmasked the transient inward current, I_T, in interneurones (Fig. 10*B*, lower traces). *I–V* relationships, averaged from a larger sample of interneurones ($n = 5$), demonstrated the overlapping range of activation of outward and of inward current, recorded under control conditions and during the action of 4-AP, respectively (Fig. 10*C*). In relay neurones ($n = 7$), 4-AP resulted in a significant increase in the amplitude of inward current positive to −50 mV, reflecting an increasing contribution of I_A to the net membrane current at these potentials (Fig. 10*B* and *C*).

In conclusion, the marked overlap in the voltage-dependent properties of I_A and I_T in interneurones tends to result in a functional compensation in terms of net membrane current, thereby presumably preventing the generation of a low-threshold Ca^{2+} action potential. Following from this, interneurones are expected to generate a regenerative Ca^{2+} response under conditions that sufficiently reduce the influence of the counteracting K^+ conductance. Indeed, during whole-cell recordings

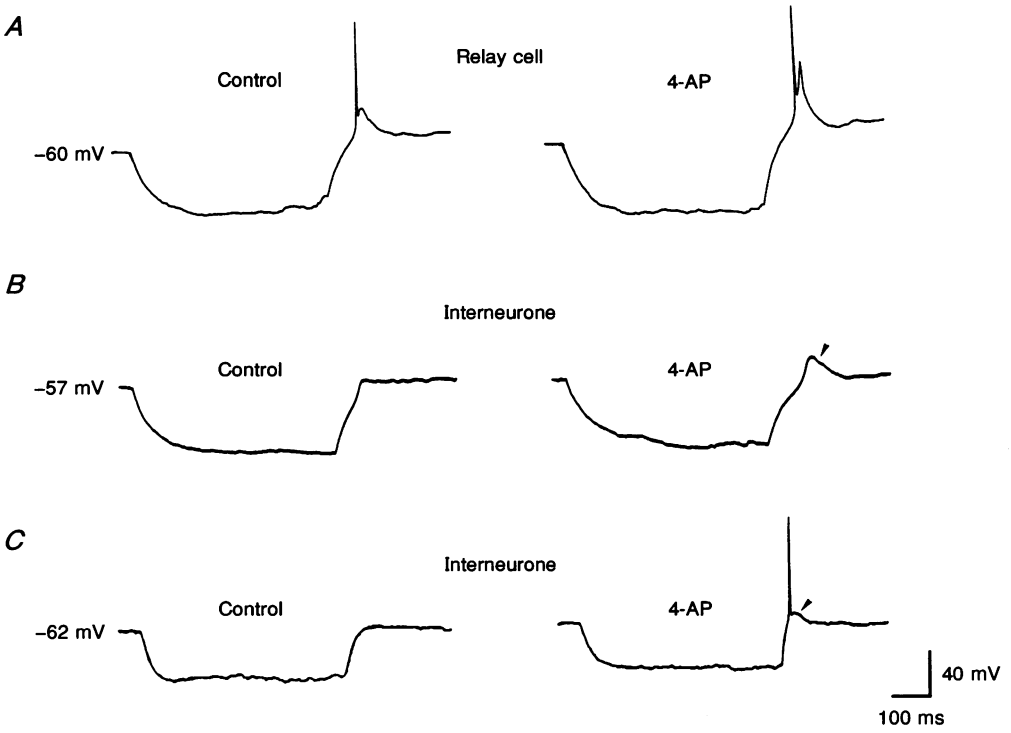

Figure 11. Consequences of I_A–I_T interactions for the generation of low-threshold regenerative Ca^{2+} responses

Whole-cell responses to hyperpolarizing current pulses (500 ms duration) obtained under current-clamp conditions from a relay cell (*A*) and two interneurones (*B* and *C*). Initial values of the membrane potential as indicated. Upon termination of the hyperpolarizing current pulse, the relay cell generates the typical Ca^{2+} action potential with a low threshold of activation crowned by a fast spike, whereas the interneurones lack a clear rebound response. External 4-AP (6 mM) results in an increase in amplitude of the Ca^{2+} action potential in the relay cell, and in a regenerative rebound response with a low threshold of activation in the interneurones (arrowheads), capable of triggering a fast spike.

under current-clamp conditions from isolated local circuit neurones we observed that blocking I_A through 4-AP unmasked a regenerative membrane depolarization with a low threshold of activation resembling the typical Ca^{2+} action potential, and which could trigger fast spikes (Fig. 11*B* and *C*; $n = 4$). In relay neurones, by comparison, the balance between the two opposing membrane conductances seems to be shifted in the direction of the voltage-dependent Ca^{2+} inward current and resulting low-threshold Ca^{2+} spike, with I_A contributing at more positive potentials, for example to repolarization of the Ca^{2+} response (cf. Jahnsen & Llinás, 1984*b*; Huguenard *et al.* 1991). In support of this hypothesis, the Ca^{2+} action potential produced by isolated relay neurones was substantially increased in amplitude and duration during blockade of I_A through 4-AP (Fig. 11*A*; $n = 5$). Activation of I_A in relay neurones may thus function to regulate the time course and amplitude of the low-threshold Ca^{2+} response rather than to prevent its generation.

DISCUSSION

Functional identity of acutely dissociated LGN neurones

The cellular morphology and synaptic connectivity of neurones in the rat LGN have been extensively studied, and the existence of two separate neuronal classes is well established (Grossman, Liebermann & Webster, 1973; Ohara *et al.* 1983; Gabbott *et al.* 1986): cortically projecting relay neurones (Golgi class A cells) are GABA/GAD immunonegative and possess a relatively large soma (mean diameter, 15–20 μm) of a multipolar or multitufted appearance, whilst the local circuit neurones (class B or type II cells) react positively for the presence of GABA or GAD and possess a small bipolar cell body (mean somatic diameter, 8–14 μm) giving rise to two long and relatively unbranched dendrites. A combination of experimental results of the present study indicates that these two classes of neurones from the rat LGN are distinguishable after acute isolation. (i) In a population of freshly dissociated cells, two morphologically different cell types are easily seen: cells possessing a relatively large multipolar cell body, and bipolar cells with elongated, smaller somata. (ii) The mean soma diameter of isolated multipolar neurones (17 μm) is within the range of that from class A neurones, and isolated bipolar neurones possess a mean soma diameter (11 μm) typical of class B neurones. (iii) Only the small bipolar cells are GABA/GAD immunoreactive, whilst the large multipolar neurones are GABA/GAD immunonegative. (iv) The size–frequency distribution of the somatic profiles is similarly bimodal for freshly dissociated bipolar and multipolar neurones, for isolated GABA/GAD-positive and GABA/GAD-negative cells, and for Nissl-stained bipolar and multipolar neurones in isolation. (v) The relative proportions of freshly dissociated bipolar neurones (17·4%), GABA/GAD-positive neurones (20·6%) and bipolar neurones after Nissl staining (19·2%) in isolation are a good representation of the contribution of GABAergic local circuit neurones to the total neuronal population of the rat LGN (18–25%; Gabbott *et al.* 1986).

The conclusion that the two classes of freshly dissociated LGN neurones represent local circuit and relay cells is supported by their basic electrogenic behaviour: the Ca^{2+}-mediated action potential with a low threshold of activation triggering fast spikes and the delay in onset to tonic firing observed in isolated multipolar neurones are properties typical of thalamocortical relay neurones (Jahnsen & Llinás, 1984*a*, *b*; Crunelli *et al.* 1987; McCormick & Pape, 1988), whilst the lack of these response parameters in dissociated bipolar cells is indicative of intrageniculate interneurones (McCormick & Pape, 1988; McCormick *et al.* 1992). These results also suggest that the basic electrophysiological properties of these cells are well preserved after enzymatic isolation.

I_T and I_A as determinants of electrical activity in local circuit neurones and relay cells

Both classes of isolated LGN neurones possess at least two voltage-dependent membrane currents, which operate in a range of membrane potentials subthreshold to the generation of Na^+–K^+-mediated action potentials: the T-type Ca^{2+} current and the A-type K^+ current. Our analysis of I_A and I_T characteristics, using the same experimental approach in isolated and identified relay cells and GABAergic local circuit neurones, allows us to discuss comparatively the degree of balance between the two opposing conductances and thereby to extrapolate their significance for electrogenic activity.

In *local circuit interneurones*, the marked similarities in the voltage-dependent properties of I_T and I_A tend to result in a functional compensation in terms of net membrane current. In particular, the ranges of steady-state inactivation of I_T and I_A are largely overlapping ($V_h = -81{\cdot}1$ *vs.* $-82{\cdot}8$ mV; $k = 4{\cdot}6$ *vs.* $8{\cdot}3$ mV^{-1}, respectively), both currents activate at around -70 mV, and they rapidly increase in amplitude with further depolarization. The net result of the combined activation is a small membrane outward current (Fig. 10*Ba*), indicating a slight dominance of I_A, and the Ca^{2+} entry through T-channels may relate to the regulation of metabolic functions rather than directly to membrane excitability (McCobb & Beam, 1991). The use of 4-AP to block I_A unmasks the Ca^{2+} inward current (Fig. 10*Ca*), corroborating the largely overlapping range of operation and the delicate functional balance between the two opposing conductances. The steep voltage dependence of activation and the relative size of I_T, which are similar to those in relay cells, will then support a regenerative membrane depolarization with properties indicative of the low-threshold Ca^{2+} action potential (Fig. 11*B* and *C*). Interestingly, the T-type Ca^{2+} current in GABAergic local circuit neurones is in many ways similar

to that in relay neurones (e.g. fast time course of activation, inactivation with voltage-dependent time constants between 40 and 20 ms, recovery from inactivation with τ around 200 ms, decrease in amplitude when Ba^{2+} is substituted for Ca^{2+} as main charge carrier). It thereby clearly differs from the Ca^{2+} current with a low threshold of activation, I_{Ts}, which has recently been described in GABAergic neurones of the reticular thalamic nucleus (characterized by slow activation kinetics, voltage-independent rate of inactivation with τ around 90 ms, slow re-activation – τ around 600 ms – and an increase in amplitude when Ba^{2+} is substituted for Ca^{2+}; Huguenard & Prince, 1992). In *relay cells*, the inactivation curve of I_T is negatively shifted along the voltage axis by almost 20 mV compared with that of I_A ($V_h = -86{\cdot}1$ *vs.* $-69{\cdot}2$ mV; $k = 4{\cdot}9$ *vs.* $7{\cdot}0$ mV^{-1}), the activation threshold for I_T (at -80 mV) is 20 mV more negative than that for I_A, and the voltage-dependent activation of I_T is steeper than that of I_A ($k = -4{\cdot}9$ *vs.* $-14{\cdot}3$ mV^{-1}). These factors promote a shift in the balance between the two opposing membrane currents toward I_T; the net current during small depolarizing steps from negative membrane potentials is largely identical with the T-type Ca^{2+} current (Fig. 10*Bb*), while I_A contributes at potentials positive to -60 mV in shaping the form and amplitude of the resulting Ca^{2+} action potential (Fig. 11*A*; cf. Huguenard *et al.* 1991). It is important to note that during the experiments that directly compare the contribution of I_A and I_T to the net membrane response, addition of 4-AP was the only experimental step employed, and at the concentration used (6 mM) 4-AP blocked I_A completely with no indication of time- or voltage-dependent unblocking (Numann, Wadman & Wong, 1987; see also Huguenard *et al.* 1991; Budde *et al.* 1992) or influences on the properties of I_T (data not shown). Another consideration relates to the temperature dependence of the membrane conductances. While similar temperature coefficients have been found in thalamic relay neurones for the rate constants of I_A and I_T inactivation/activation (Q_{10} at around 3), the amplitude of I_T ($Q_{10} = 3{\cdot}1$) is more dependent on temperature than that of I_A ($Q_{10} = 1{\cdot}6$; Coulter *et al.* 1989; Huguenard *et al.* 1991). An increase in temperature (i.e. from room temperature to more physiological values) would thus result in a relatively larger increase in amplitude of I_T than that of I_A. The temperature coefficients for the respective conductances in GABAergic local circuit neurones are unknown, and exact functional consequences for the I_T/I_A balance in the two classes of neurones cannot be deduced from available data. However, recordings performed at 37 °C in the slice preparation of the LGN demonstrated the presence of a strong Ca^{2+}-mediated action potential in relay neurones (Jahnsen & Llinás, 1984*a*, *b*), whereas a clear regenerative Ca^{2+} response with a low threshold of activation was absent in interneurones under normal conditions, but it could be unmasked through application of 4-AP (McCormick & Pape, 1988; H. C. Pape & D. A. McCormick, unpublished observations), thereby confirming the distinct functional balance between I_A and I_T in the two classes of LGN neurones.

The difference in the steady-state inactivating properties of I_T and I_A in *relay neurones* creates a range of membrane potentials around -70 mV, where I_T is fully inactivated, whilst I_A is (partly) de-inactivated. Depolarizing influences acting on relay neurones at this range of membrane potentials will tend to activate a transient K^+ outward current, I_A (with no contribution of an opposing Ca^{2+} current, I_T), thereby imposing the typical delay on the onset of action potential discharges (cf. Jahnsen & Llinás, 1984*b*; McCormick & Pape, 1988; Budde *et al.* 1992). In *local circuit neurones*, a range of membrane potentials for selective activation of I_A seems not to exist, due to the large overlap in the voltage-dependent characteristics of I_A and I_T, and interneurones are indeed not observed to produce a delay to the onset to spike firing under normal conditions (Fig. 3*A*; cf. McCormick & Pape, 1988). While these conclusions support the notion of an important role of I_A in controlling the excitability of thalamic neurones at membrane potentials near rest (Huguenard *et al.* 1991; Budde *et al.* 1992), additional slowly inactivating components of K^+ current may contribute to the modulation of the firing threshold in the long-term range (Huguenard & Prince, 1991; McCormick, 1991; Budde *et al.* 1992). A striking difference between I_A and I_T relates to the time course of recovery from inactivation. The fast kinetics of I_A in *relay cells* ($\tau = 21$ ms, compared with $\tau = 206$ ms for I_T) will promote the selective de-inactivation of I_A during hyperpolarizing membrane responses of a short duration, for example during the hyperpolarizing after-potential following a single Na^+–K^+-mediated action potential, thereby supporting the classic role of I_A in enabling slow repetitive firing (Connor & Stevens, 1971; Rudy, 1988; Huguenard *et al.* 1991). In *interneurones*, the more negative range of inactivation and the prolonged time course of recovery from inactivation ($\tau = 77$ ms) tend to prevent this function of I_A, which in turn may contribute to the tonic high-frequency discharges observed in GABAergic local circuit neurones (McCormick & Pape, 1988).

Functional implications of Ca^{2+}-mediated regenerative activity in thalamic circuits

The T-type Ca^{2+} current and the resulting low-threshold Ca^{2+} action potential crowned by a high-frequency burst of Na^+–K^+-mediated spikes are considered as important elements in the generation of rhythmic oscillatory burst activity in thalamocortical circuits (for reviews, see Steriade *et al.* 1990; McCormick, 1992). This oscillatory bursting in turn provides an important mechanism in the generation of synchronized oscillatory activity in the forebrain, which is represented as spindling oscillations and slow/delta waves in the electroencephalogram (EEG) during the early and late stages of slow-wave sleep (Steriade & Deschênes, 1984; Steriade, Curró Dossi & Nuñez,

1991; Curró Dossi, Nuñez & Steriade, 1992). Spindling oscillation seems to rely on thalamic network properties, in that Ca^{2+}-mediated bursts are produced in thalamocortical neurones as rebound responses arising from rhythmically reoccurring IPSPs mediated through GABAergic reticular thalamic neurones (Steriade, Deschênes, Domich & Mulle, 1985; Von Krosigk, Bal & McCormick, 1993). Delta oscillation results, for the most part, from the capability of thalamocortical neurones to function as intrinsic oscillators, which rhythmically (0·5–4 Hz) produce Ca^{2+}-mediated action potentials largely due to an intrinsic interaction between I_T and a hyperpolarization-activated cation current, I_h (McCormick & Pape, 1990; Soltesz, Lightowler, Leresche, Jassik-Gerschenfeld, Pollard & Crunelli, 1991). Although the exact mechanisms that regulate the different types of oscillatory behaviour and synchronize the neuronal oscillators in the thalamus are unclear at present, the prevailing membrane potential and the influence of corticothalamic fibres seem to be important. A series of experiments performed in the cat *in vivo* (Nuñez, Curró Dossi, Contreras & Steriade, 1992) demonstrated that spindle oscillations in thalamocortical neurones occurred at membrane potentials at or slightly negative to the normal resting value (between −55 and −65 mV), whereas delta oscillations appeared in more hyperpolarized regions of the membrane, that is, within the range of de-inactivation/activation of I_T and I_h. Electrical stimulation of the corticothalamic pathway (Steriade *et al.* 1991) could induce long-lasting IPSPs in thalamocortical cells, giving rise to slow rhythmic burst activity within the frequency range of delta oscillation; it could potentiate slow/delta oscillations in thalamocortical cells, and the slow rhythmic burst activity of previously unrelated cells could become synchronized after a series of corticothalamic volleys. From these findings it was concluded that the deepening of EEG-synchronized sleep is associated with a membrane hyperpolarization in thalamocortical relay neurones, which in turn enables slow rhythmic burst activity, and that the thalamocorticothalamic loop functions to reinforce the oscillation. GABAergic neurones in the thalamus were proposed to represent important targets of the reinforcing corticothalamic input, in that they provide phase-locked hyperpolarizing influences on rhythmically active relay neurones necessary to sustain and synchronize slow/delta burst activity. The anatomical demonstration (Weber, Kalil & Behan, 1989) that corticogeniculate terminals synapse primarily with GABAergic neurones in the LGN is in line with this notion. The data of the present study demonstrate for the first time that GABAergic local circuit cells in the thalamus do possess the T-type Ca^{2+} conductance, and hence the basic membrane mechanism underlying low-threshold burst activity. The expression of burst firing, however, seems to be preventable by the delicate functional balance between I_T and the fast transient K^+ current, I_A. That activation of I_A prevents burst firing has also been suggested in other systems, such as Betz cells in the cortex (Schwindt, Spain, Foehring, Stafstrom, Chubb & Crill, 1988) or neurones in the brainstem (Gerber, Greene & McCarley, 1989; Kang & Kitai, 1990; Leonard & Llinás, 1990). From this it is tempting to speculate that regulatory influences are capable of shifting the balance between the two opposing membrane currents, thereby, for example, selectively inducing burst activity in interneurones and supporting their function in synchronizing slow oscillatory burst firing of the synaptic network. Three observations are in line with this idea: (i) the presence of a regenerative Ca^{2+} response with a low threshold of activation during the action of 4-AP in local circuit neurones in the cat LGN slice *in vitro* (H. C. Pape & D. A. McCormick, unpublished observations), (ii) the generation of rebound burst activity following membrane hyperpolarization by a subpopulation of local circuit neurones in the cat LGN *in vitro* (McCormick *et al.* 1992), and (iii) the occurrence of long bursts of spikes in presumed interneurones of the rat LGN *in vivo* (Burke & Sefton, 1966). In view of the numerical predominance of corticofugal terminals on GABAergic cells and the importance of the corticothalamic loop in reinforcing oscillatory burst activity in the thalamus, it is interesting to note that excitatory amino acids acting on metabotropic glutamate receptors have been shown to participate in corticothalamic transmission (Streit, 1984; McCormick & Von Krosigk, 1992). Metabotropic glutamate receptors are linked to intracellular messenger systems controlling a broad range of cellular parameters such as internal Ca^{2+} mobilization and K^+ channel function (as reviewed by Baskys, 1992), and they may well provide the elements involved in the control of the functional balance in GABAergic local circuit cells. Indeed, stimulation of metabotropic glutamate receptors in hippocampal inhibitory interneurones could transform the firing pattern from a discharge of single action potentials to rhythmic burst activity, resulting in rhythmically occurring IPSPs in pyramidal neurones (Miles & Poncer, 1993). In the LGN, the engagement of GABAergic local circuit cells may support synchronizing influences exerted by recurrent connections from the perigeniculate sector of the reticular thalamic nuclear complex (Amzica, Nuñez & Steriade, 1992) and by axon collaterals of relay cells within the main layers of the LGN (Soltesz & Crunelli, 1992), thereby stabilizing and synchronizing the slow/delta oscillation observed during the deepening of EEG-synchronized sleep, or contributing to the abnormal rhythmicity characterizing certain forms of generalized epilepsy (Liu, Vergnes, Depaulis & Marescaux, 1991; Hosford *et al.* 1992).

REFERENCES

Ahlsén, G., Lindström, S. & Lo, F.-S. (1984). Inhibition from the brain stem of inhibitory interneurones of the cat's dorsal lateral geniculate nucleus. *Journal of Physiology* **347**, 593–609.

Amzica, F., Nuñez, A. & Steriade, M. (1992). Delta frequency (1–4 Hz) oscillations of perigeniculate thalamic neurons and their modulation by light. *Neuroscience* **51**, 285–294.

BASKYS, A. (1992). Metabotropic receptors and 'slow' excitatory actions of glutamate agonists in the hippocampus. *Trends in Neurosciences* **15**, 92–96.

BUDDE, T., MAGER, R. & PAPE, H.-C. (1992). Different types of potassium outward current in relay neurons acutely isolated from the rat lateral geniculate nucleus. *European Journal of Neuroscience* **4**, 708–722.

BURKE, W. & SEFTON, J. (1966). Discharge patterns of principal cells and interneurones in lateral geniculate nucleus of rat. *Journal of Physiology* **187**, 201–212.

CONNOR, J. A. & STEVENS, C. F. (1971). Voltage clamp studies of a transient outward current in gastropod neural somata. *Journal of Physiology* **215**, 21–30.

COULTER, D. A., HUGUENARD, J. R. & PRINCE, D. A. (1989). Calcium currents in rat thalamocortical relay neurones: kinetic properties of the transient, low-threshold current. *Journal of Physiology* **414**, 587–604.

CRUNELLI, V., KELLY, J. S., LERESCHE, N. & PIRCHIO, M. (1987). The ventral and dorsal lateral geniculate nucleus of the rat: intracellular recordings *in vitro*. *Journal of Physiology* **384**, 587–601.

CRUNELLI, V. & LERESCHE, N. (1991). A role of $GABA_B$ receptors in excitation and inhibition of thalamocortical cells. *Trends in Neurosciences* **14**, 16–21.

CRUNELLI, V., LIGHTOWLER, S. & POLLARD, C. E. (1989). A T-type Ca^{2+} current underlies low-threshold Ca^{2+} potentials in cells of the cat and rat lateral geniculate nucleus. *Journal of Physiology* **413**, 543–561.

CURRÓ DOSSI, R., NUÑEZ, A. & STERIADE, M. (1992). Electrophysiology of a slow (0·5–4 Hz) intrinsic oscillation of cat thalamocortical neurones *in vivo*. *Journal of Physiology* **447**, 215–234.

DUBIN, W. M. & CLELAND, B. G. (1977). Organization of visual inputs to interneurons of lateral geniculate nucleus of the cat. *Journal of Neurophysiology* **40**, 410–427.

FITZPATRICK, D., PENNY, G. R. & SCHMECHEL, D. E. (1984). Glutamic acid decarboxylase-immunoreactive neurons and terminals in the lateral geniculate nucleus of the cat. *Journal of Neuroscience* **4**, 1809–1829.

GABBOTT, P. L. A., SOMOGYI, J., STEWARD, M. G. & HAMORI, J. (1986). GABA-immunoreactive neurons in the dorsal lateral geniculate nucleus of the rat: characterisation by combined Golgi-impregnation and immunocytochemistry. *Experimental Brain Research* **61**, 311–322.

GERBER, U., GREENE, R. W. & MCCARLEY, R. W. (1989). Repetitive firing properties of medial pontine reticular formation neurones of the rat recorded *in vitro*. *Journal of Physiology* **410**, 533–560.

GROSSMANN, A., LIEBERMANN, A. R. & WEBSTER, K. E. (1973). A Golgi study of the rat dorsal lateral geniculate nucleus. *Journal of Comparative Neurology* **150**, 441–466.

GUILLERY, R. W. (1966). A study of Golgi preparations from the dorsal lateral geniculate nucleus of the adult cat. *Journal of Comparative Neurology* **128**, 21–50.

HAMILL, O. P., MARTY, A., NEHER, E., SAKMANN, B. & SIGWORTH, F. (1981). Improved patch-clamp techniques for high-resolution current recording from cells and cell-free membrane patches. *Pflügers Archiv* **391**, 85–100.

HERNÁNDEZ-CRUZ, A. & PAPE, H.-C. (1989). Identification of two calcium currents in acutely dissociated neurons from the rat lateral geniculate nucleus. *Journal of Neurophysiology* **61**, 1270–1283.

HOSFORD, D. A., CLARK, S., CAO, Z., WILSON, W. A. JR, LIN, F., MORRISETT, R. A. & HUIN, A. (1992). The role of $GABA_B$ receptor activation in absence seizures of lethargic (*lh/lh*) mice. *Science* **257**, 398–401.

HUGUENARD, J. R., COULTER, D. A. & PRINCE, D. A. (1991). A fast transient potassium current in thalamic relay neurons: kinetics of activation and inactivation. *Journal of Neurophysiology* **66**, 1304–1315.

HUGUENARD, J. R. & PRINCE, D. A. (1991). Slow inactivation of a TEA-sensitive K^+ current in acutely isolated rat thalamic relay neurons. *Journal of Neurophysiology* **66**, 1316–1328.

HUGUENARD, J. R. & PRINCE, D. A. (1992). A novel T-type current underlies prolonged Ca^{2+}-dependent burst firing in GABAergic neurons of rat thalamic reticular nucleus. *Journal of Neuroscience* **12**, 3804–3817.

JAHNSEN, H. & LLINÁS, R. (1984*a*). Electrophysiological properties of guinea-pig thalamic neurones: an *in vitro* study. *Journal of Physiology* **349**, 205–226.

JAHNSEN, H. & LLINÁS, R. (1984*b*). Ionic basis for the electroresponsiveness and oscillatory properties of guinea-pig thalamic neurones *in vitro*. *Journal of Physiology* **349**, 227–247.

JONES, E. G. (1985). *The Thalamus*. Plenum Publishing Corporation, New York.

KANG, Y. & KITAI, S. T. (1990). Electrophysiological properties of pedunculopontine neurons and their postsynaptic responses following stimulation of substantia nigra reticulata. *Brain Research* **535**, 79–95.

KAY, A. L. & WONG, R. K. S. (1986). Isolation of neurons suitable for patch-clamping from adult mammalian central nervous systems. *Journal of Neuroscience Methods* **16**, 227–238.

LEONARD, C. S. & LLINÁS, R. (1990). Electrophysiology of mammalian pedunclopontine and lateral dorsal tegmental neurones in vitro: implications for the control of REM sleep. In *Brain Cholinergic Systems*, ed. STERIADE, M. & BIESOLD, D., pp. 205–223. Oxford University Press, Oxford, New York.

LIU, Z., VERGNES, M., DEPAULIS, A. & MARESCAUX, C. (1991). Evidence for a critical role of GABAergic transmission within the thalamus in the genesis and control of absence seizures in the rat. *Brain Research* **545**, 1–7.

MCCOBB, D. P. & BEAM, K. G. (1991). Action potential waveform voltage-clamp commands reveal striking differences in calcium entry via low and high voltage-activated calcium channels. *Neuron* **7**, 119–127.

MCCORMICK, D. A. (1991). Functional properties of a slowly inactivating potassium current in guinea-pig dorsal lateral geniculate relay neurons. *Journal of Neurophysiology* **66**, 1176–1189.

MCCORMICK, D. A. (1992). Neurotransmitter actions in the thalamus and the cerebral cortex and their role in neuromodulation of thalamocortical activity. *Progress in Neurobiology* **39**, 337–388.

MCCORMICK, D. A. & PAPE, H.-C. (1988). Acetylcholine inhibits identified interneurons in the cat lateral geniculate nucleus. *Nature* **334**, 246–248.

MCCORMICK, D. A. & PAPE, H.-C. (1990). Properties of a hyperpolarization-activated cation current and its role in rhythmic oscillation in thalamic relay neurones. *Journal of Physiology* **431**, 291–318.

MCCORMICK, D. A., PAPE, H.-C., KISVÁRDAY, Z. & EYSEL, U. T. (1992). Electrophysiological and pharmacological properties of LGNd interneurons. *Society for Neuroscience Abstracts* **18**, 212.

MCCORMICK, D. A. & VON KROSIGK, M. (1992). Corticothalamic activation modulates thalamic firing through glutamate "metabotropic" receptors. *Proceedings of the National Academy of Sciences of the USA* **89**, 2774–2778.

MILES, R. & PONCER, J. C. (1993). Metabotropic glutamate receptors mediate a post-tetanic excitation of guinea-pig hippocampal inhibitory interneurones. *Journal of Physiology* **463**, 461–473.

MONTERO, V. M. & SINGER, W. (1985). Ultrastructural identification of somata and neural processes immunoreactive to antibodies against glutamic acid decarboxylase (GAD) in the dorsal lateral geniculate nucleus of the cat. *Experimental Brain Research* **59**, 151–165.

NUMANN, R. E., WADMAN, W. J. & WONG, R. K. S. (1987). Outward currents in single hippocampal cells obtained from the adult guinea-pig. *Journal of Physiology* **393**, 331–353.

NUÑEZ, A., CURRÓ DOSSI, R., CONTRERAS, D. & STERIADE, M. (1992). Intracellular evidence for incompatibility between spindle and delta oscillations in thalamocortical neurons of cat. *Neuroscience* **48**, 75–85.

OHARA, P. T., LIEBERMAN, A. R., HUNT, S. P. & WU, J.-Y. (1983). Neural elements containing glutamic acid decarboxylase (GAD) in the dorsal lateral geniculate nucleus of the rat: immunohistochemical studies by light and electron microscopy. *Neuroscience* **8**, 189–211.

RUDY, B. (1988). Diversity and ubiquity of K^+ channels. *Neuroscience* **25**, 729–749.

SCHWINDT, P. C., SPAIN, W. J., FOEHRING, R. C., STAFSTROM, C. E., CHUBB, M. C. & CRILL, W. E. (1988). Multiple potassium conductances and their functions in neurons from cat sensorimotor cortex in vitro. *Journal of Neurophysiology* **59**, 424–449.

SOLTESZ, I. & CRUNELLI, V. (1992). A role for low-frequency, rhythmic synaptic potentials in the synchronization of cat thalamocortical cells. *Journal of Physiology* **457**, 257–276.

SOLTESZ, I., LIGHTOWLER, S., LERESCHE, N., JASSIK-GERSCHENFELD, D., POLLARD, C. E. & CRUNELLI, V. (1991). Two inward currents and the transformation of low-frequency oscillations in rat and cat thalamocortical cells. *Journal of Physiology* **441**, 175–197.

STERIADE, M., CURRÓ DOSSI, R. & NUÑEZ, A. (1991). Network modulation of a slow intrinsic oscillation of cat thalamocortical neurons implicated in sleep delta waves: cortically induced synchronisation and brainstem cholinergic suppression. *Journal of Neuroscience* **11**, 3200–3217.

STERIADE, M. & DESCHÊNES, M. (1984). The thalamus as a neuronal oscillator. *Brain Research Reviews* **8**, 1–63.

STERIADE, M., DESCHÊNES, M., DOMICH, L. & MULLE, C. (1985). Abolition of spindle oscillations in thalamic neurons disconnected from nucleus reticularis thalami. *Journal of Neurophysiology* **54**, 1473–1497.

STERIADE, M., JONES, E. G. & LLINÁS, R. R. (1990). *Thalamic Oscillations and Signaling*. John Wiley & Sons, New York.

STERLING, P. & DAVIS, T. L. (1980). Neurons in cat lateral geniculate nucleus that concentrate exogenous [^{3}H]-γ-amino-butyric acid (GABA). *Journal of Comparative Neurology* **192**, 737–749.

STREIT, P. (1984). Glutamate and aspartate as transmitter candidates for systems of the cerebral cortex. In *Cerebral Cortex*, vol. 2, *Functional Properties of Cortical Cells*, ed. JONES, E. G. & PETERS, A., pp. 119–143. Plenum Press, New York.

SUZUKI, S. & ROGAWSKI, M. A. (1989). T-type calcium channels mediate the transition between tonic and phasic firing in thalamic neurons. *Proceedings of the National Academy of Sciences of the USA* **86**, 7228–7232.

VON KROSIGK, M., BAL, T. & MCCORMICK, D. A. (1993). Cellular mechanisms of a synchronized oscillation in the thalamus. *Science* **261**, 361–364.

WEBER, A. J., KALIL, R. E. & BEHAN, M. (1989). Synaptic connections between corticogeniculate axons and interneurons in the dorsal lateral geniculate nucleus of the cat. *Journal of Comparative Neurology* **289**, 156–164.

Acknowledgements

The authors would like to thank Dr U. Eysel for support, Mrs C. Schlauß and Mrs E. Tóth for technical assistance, Mrs P. Hentrich for help with the analysis of soma areas of isolated cells, and Mrs D. Strehler for the photographs in Fig. 1. This research was supported by a grant from the Deutsche Forschungsgemeinschaft to H.-C. P. (Ey 8/17–2).

Received 23 August 1993; accepted 17 December 1993.